Electronic Supplementary Information

Pore-space-partitioned and hetero-atom enriched dual-redox scalable metal-organic framework synergistically boosts overall water splitting

Bapan Maji [a,b], Sreenivasan Nagappan† [a,c], Rudra Chand† [a,b], Dipankar Das[a,d], Bishwajit Ganguly[a,d,],Subrata Kundu[a,c,*], Subhadip Neogi[a, b, *]

[a]Academy of Scientific and Innovative Research (AcSIR), Ghaziabad- 201002, India
[b]Inorganic Materials & Catalysis Division, CSIR-Central Salt & Marine Chemicals Research Institute, Bhavnagar, Gujarat 364002, India
[c]Electrochemical Process Engineering (EPE) Division, CSIR−Central Electrochemical Research Institute (CECRI), Karaikudi, Tamil Nadu 630003, India
[d]Computational and Simulation Unit (Marine Elements and Marine Environment Division and Centralized Instrument Facility), CSIR-Central Salt & Marine Chemicals Research Institute, Bhavnagar-364002, Gujarat, India.

*_E-mail_: skundu@cecri.res.in (S. Kundu), sneogi@csmcri.res.in, subhadip79@gmail.com (S. Neogi)

Table of Contents

Section S1. Materials and Physical measurements

All the solvents and reagents were purchased from commercially available sources (except DPTz) and used without further purification. Powder X-ray diffraction (PXRD) data were collected using a RIGAKU MINIFLEX X-ray diffractometer (2θ=10-80°). Thermogravimetric analyses (TGA) (heating rate of 5 °C/min under N_2 atmosphere) were performed with a Mettler Toledo Star SW 8.10 system. The Fourier Transform Infrared spectra (FT-IR) of the samples were recorded using the KBr pellet method on a Perkin–Elmer GX FTIR spectrometer in the region of 4000−400 cm^{-1}. ^{1}H and ^{13}C NMR spectra were recorded on a Bruker Avance-II 500 MHz NMR spectrometer. Scanning Electron Microscopic (SEM) and Transmission Electron Microscopic (TEM) images were obtained using a JEOL JSM 7100F and a JEOL JEM 2100 instrument, respectively. XPS analysis was carried out using a Thermo Scientific ESCALAB 250 Xi photoelectron spectrometer (XPS) using a monochromatic Al Kα X-ray as an excitation. The surface area and CO_2 adsorption measurement was carried out using the Quantachrome Autosorb IQ instrument.

Section S2. Single Crystal X-ray Crystallography

Single crystals with suitable dimensions were chosen under an optical microscope and mounted on a glass fibre for data collection. The crystal data for the as-synthesized crystal of FCG-11 were collected on a Bruker D8 Quest diffractometer, with a CMOS detector in shutterless mode. The crystal data were collected at room temperature. The instrument was equipped with a graphite monochromatized Mo Kα X-ray source (λ = 0.71073 Å), with Triumph™ X-ray source optics. Data collection, initial indexing and cell refinement were handled using APEX II software.[1] Frame integration, including Lorentz polarization corrections, and final cell parameter calculation were carried out using SAINT+ software.[2] The data were corrected for absorption using the SADABS program.[3] The decay of reflection intensity was monitored by analysis of redundant frames. The structure was solved using Direct methods and different Fourier techniques. All non-hydrogen atoms were refined anisotropically. All H atoms were placed in calculated positions using idealized geometries (riding model) and assigned fixed isotropic displacement parameters. The SHELXL-2014 package within the OLEX2 crystallographic software was applied for structure refinement with several full-matrix least-squares/difference Fourier cycles. The disordered guest solvent molecules in the crystal lattice were treated with the solvent mask option in OLEX2 software.[4] The potential solvent-accessible void space was calculated using the PLATON software.[5] The crystal and refinement data for solvent-free FCG-11 are listed in Table S1. Topological analysis was performed by using TOPOS software.[6]

Section S3. Electrochemical Characterizations for the three-electrode system.

Electrochemical measurements: The electrochemical properties were measured using a Metrohm AUTOLAB-M240 instrument with techniques like CV, LSV, and EIS. All the electrochemical experiments were carried out by employing a conventional three-electrode set-up. (Hg/HgO reference (1 M KOH internal solution), carbon cloth-counter and carbon fiber (CF) as working electrode). The working electrodes were fabricated using 1 mg of

polyvinylidene fluoride (PVDF) as a binder and N-Methyl-2-pyrrolidone (NMP) as a slurry preparation agent. Typically, the ≈4:1 (with respect to overall catalyst loading over the electrode surface) ratio of catalyst and PVDF was taken into a mortar, followed by the addition of NMP solvent with continuous mixing by a pestle. Then, a certain amount of catalyst ink was fabricated over the 1 cm^2 area of the carbon fiber (CF). The amount of loaded catalyst was calculated by measuring the difference in weight of coated and uncoated carbon fiber (CF). The polarization studies were carried out at a slow scan rate of 5 mV/sec. 100 % iR compensation was done manually from the R_u from EIS. The electrochemical impedance studies were carried out in the frequency range of 0.1 Hz to 100 kHz.

Overpotential

The overpotential values of all the catalysts were calculated at a benchmarking current density of 10 mA cm^{-2} by employing the following relation. The standard electrode potential of the water oxidation reaction decreases with temperature. So, when determining overpotentials (η) during OER at high temperatures (e.g., 25–70 °C), be sure to subtract the corrected E°(T) and not just the 1.23 V.

$$\eta = E_{app} - E^0(T) \quad \text{..... (E1)}$$

Tafel Slope Calculation

Tafel slope talks about the relation between the applied overpotential and current density on a log scale, and the corresponding plots are called the Tafel plot. Tafel slope values are derived from the Butler-Volmer equation, which can be represented as

$$h = b \times \log(j) + a$$

$$b = (h - a)/[\log(j)] \text{.....(E2)}$$

whereas b, h, j, and a are represented as a Tafel slope, overpotential, current density and reaction constant, respectively. Hence, equation (V) suggests that the current density is inversely proportional to the Tafel slope.

Electrochemically Active Surface Area (ECSA)

The electrochemically active surface areas (ECSA) were measured by determining the electrochemical C_{dl} using the following equations:

$i_c = \nu \times C_{dl}$ ……(E3)

$ECSA = C_{dl}/C_s$……(E4)

where "i_c" indicates the double-layer charging current resulting from scan-rates (ν) dependent CVs at non-faradic potential, and "Cs" denotes a specific capacitance value of 0.040 mF $cm^{-2,}$ depending on the typical reported values.

Mass Activity

Mass activity for the oxygen evolution reaction (OER) is calculated as the current generated per unit mass of the catalyst at a given overpotential (1.55 V vs. RHE for OER). The general formula is:

Mass Activity: $(Ag^{-1}) = \frac{j}{m}$ ……(E5)

Where:

- j is the current density measured during the OER experiment.
- m is the mass of the catalyst (g) loaded onto the electrode.

Turnover frequency (TOF)

Calculation of overpotential is quite important to determine the activity of the catalyst; apart from that, calculation of turnover frequency (TOF) is also necessary to find out the potentiality of a catalyst at a particular overpotential. TOF is simply defined as the number of moles of H_2/O_2 formed per unit time from a catalytically active site. The equation which is used to calculate the TOF value of a catalyst is given below,

$$\text{TOF}=(J_{\text{ECSA}} \times N_{\text{A}})/(\text{n} \times \text{F} \times \tau_{\text{Rh atoms per } cm^2}) \quad \ldots\ldots\ldots\ldots\text{(E6)}$$

where J is the current density at a certain overpotential, N_A is the Avogadro number, n is the number of electron transfers (OER n = 4 and HER n = 2), F is the Faraday constant, and τ is the number of active sites (Rh site) per cm² (ECSA).

Stability

Stability is a vital criterion when utilizing an electrocatalyst for the commercial production of hydrogen. To evaluate an electrode's stability, two common approaches are potentiostatic or galvanostatic tests, as well as cyclic voltammetry (CV) accelerated degradation studies. In a potentiostatic setup, the current remains fixed while the potential varies over time; conversely, in a galvanostatic setup, the current is held constant while the potential changes. A minimal change in performance of the working electrode during OER or HER indicates good stability for prolonged use. To further evaluate catalyst stability, a continuous stability study can be performed over a period ranging from 12 to 100 hours. This approach allows for a comprehensive assessment of the electrocatalyst's durability under operational conditions, ensuring that it can maintain performance over extended periods, which is crucial for practical applications in hydrogen production.

Faradaic Efficiency (FE) for OER

The FE estimated an electrode's effectiveness in producing gas by comparing the experimental amount of O_2 generated to the theoretically expected amount. The FE can be determined using:

$$FE = \frac{Experimental\ mol\ of \frac{H_2}{O_2} gas}{Theoretical\ mol\ of \frac{H_2}{O_2} gas} 100\% \quad \ldots\ldots\ldots\ldots\text{(E7)}$$

Faraday's law can calculate the theoretical value of O_2:

$$n = \frac{It}{ZF} \ldots\ldots\ldots\ldots\text{(E8)}$$

where *n* denotes the amount of theoretical product produced in mol, *I* is the current in amperes, t is the time in seconds, and z is the number of transferred electrons, i.e., O_2 (*z* = 4), respectively. The Faraday constant (*F*) is 96,485 C mol^{-1}. The theoretical values of O_2 can be calculated at 100 mA for 10 ~ 60 min. The gas produced was collected using the water-gas displacement technique**.** The quantity of O_2 can be determined using:

$$PV = nRT \quad \ldots\ldots\ldots\ldots\text{(E9)}$$

where *V* denotes the volume of collected gas, *T* denotes the temperature in kelvin, *R* denotes the ideal gas constant (0.0821 atm/mol K), and *P* denotes the atmospheric pressure (~1 atm).

Faradaic Efficiency (FE) for HER

The FE estimated an electrode's effectiveness in producing gas by comparing the experimental amount of H_2 generated to the theoretically expected amount. The FE can be determined using:

$$FE = \frac{Experimental\ mol\ of \frac{H_2}{O_2} gas}{Theoretical\ mol\ of \frac{H_2}{O_2} gas} 100\% \quad \text{……(E10)}$$

Faraday's law can calculate the theoretical value of H_2:

$$n = \frac{It}{ZF} \quad \text{……(E11)}$$

where *n* denotes the amount of theoretical product produced in mol, *I* is the current in amperes, t is the time in seconds, and z is the number of transferred electrons, i.e., H_2 ($z = 2$), respectively. The Faraday constant (*F*) is 96,485 C mol^{-1}. The theoretical values of H_2 can be calculated at 100 mA for 10 ~ 60 min. The gas produced was collected using the water-gas displacement technique.

$$PV = nRT \quad \text{……(E12)}$$

where *V* denotes the volume of collected gas, *T* denotes the temperature in kelvin, *R* denotes the ideal gas constant (0.0821 atm/mol K), and *P* denotes the atmospheric pressure (~1 atm).

TOF Value calculation

1. Calculated area associated with the reduction of Co^{2+} to Co^{3+} of FCG-11 = 0.000014770770496544 VA

Hence, the associated charge is = 0.000014770770496544 VA / 0.005 Vs^{-1}

= 0.002954154 As

= 0.002954154 C

Now, the number of electrons transferred is = 0.002954154 C / 1.602 $\times 10^{-19}$

= 1.84404×10^{16}

Since the reduction of Co^{3+} to Co^{2+} is a single-electron transfer reaction, the number of electrons calculated above is the same as the number of surface-active sites.

Hence, the number of Co that participate in OER is = 1.84404×10^{16}

Determination of Turnover Frequency (TOF) from OER Current Density. TOF in our study was calculated assuming that the surface-active Co atoms that had undergone the redox reaction just before the onset of OER only participated in OER electrocatalysis. The corresponding expression is,

$$TOF = j \times N_A / F \times n \times \Gamma \quad \text{……. (E6)}$$

Where, j = current density, N_A = Avogadro number, F = Faraday constant, n = Number of electrons Γ = Surface concentration.

Hence, we have,

$TOF_{1.55\ V}$ = [(40.47× 10^{-3}) (6.023× 10^{23})] / [(96485) (4) (1.84404× 10^{16})]

= 3.422422193 sec^{-1}

In the same way, we have also done the calculation for others.

Section S4. Experimental section

Synthesis of 2,5-di(pyridin-4-yl) thiazolo-[5,4-d] thiazole (DPTz): Dithiooxamide (200 mg,1.6 mmol) was dissolved in 20 mL of DMF (N, N-dimethyl formamide) in a round-bottom flask, and after that, 4-pyridinecarboxaldehyde (4.4 mmol, 400µL) was added to the reaction mixture. The reaction mixture was refluxed for 4 hrs at 155 ºC. After cooling overnight, a yellow crystalline product was obtained, which was filtered and washed with DMF and Water. The product was dried in air, and characterization was done by ^{1}H NMR. (345 mg, 51.28% yield. ^{1}H NMR (500 MHz, $CDCl_3$) δ8.79- 8.77 (d, J= 5 Hz, 2H), δ 7.88-7.87 (d J =5 Hz, 2H).

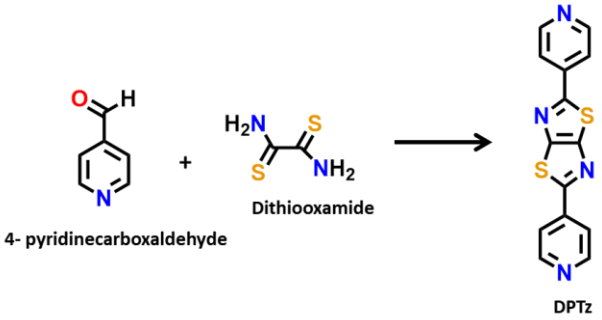

Scheme S1. Synthetic scheme of 2,5-di(pyridin-4-yl) thiazolo-[5,4-d] thiazole (DPTz) linker.

a)

b)

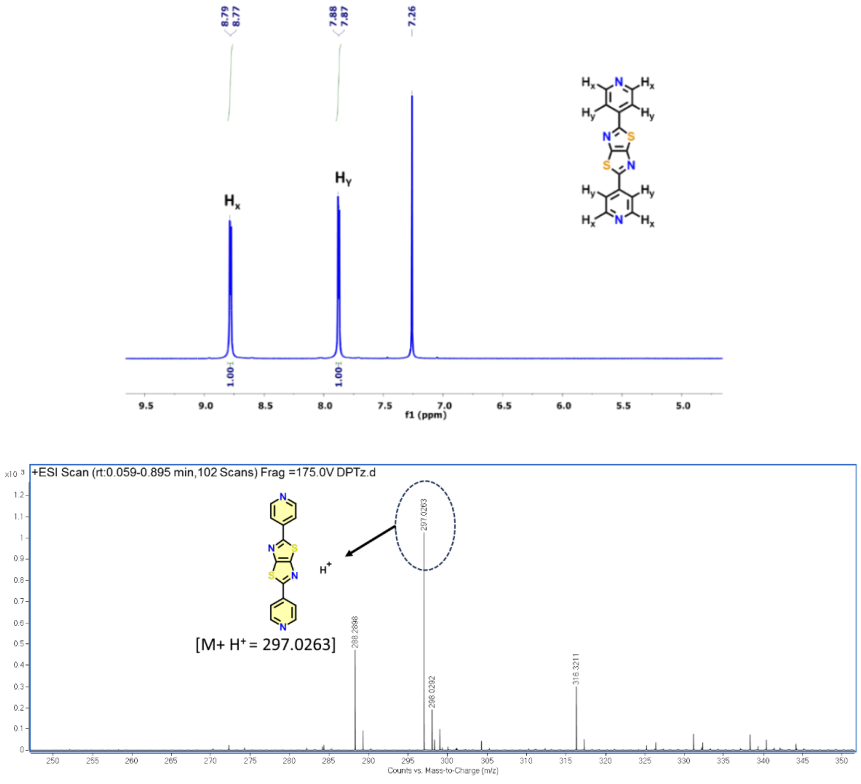

Fig. S1 (a) ^{1}H NMR of DPTz in $CDCl_3$ and (b) LC-MS analysis of DPTz.

a)

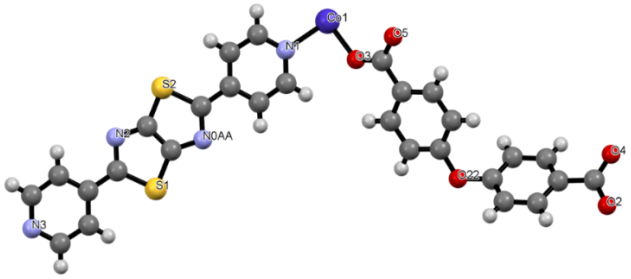

b)

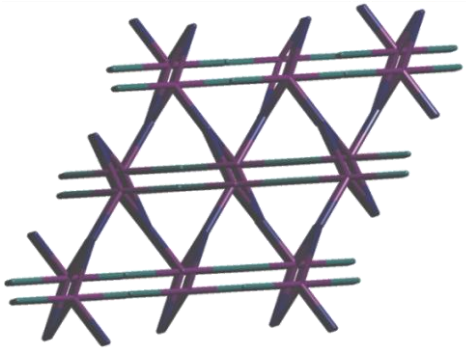

c)

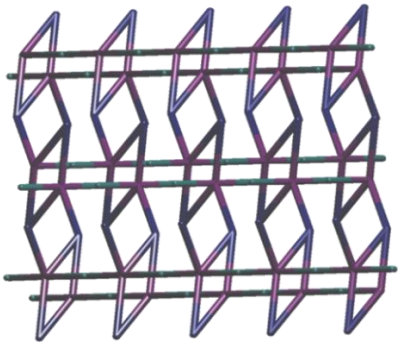

Fig. S2 (a) Asymmetric unit, and Topological representations of FCG-11 along the crystallographic (b) *a*, and (c) c axis.

Table S1. Crystal data and refinement parameters for FCG-11.

Identification code	**FCG-11**
Empirical formula	$C_{28}H_{16}CoN_4O_5S_2$
Formula weight	610.51
Temperature/K	273.15
Crystal system	monoclinic
Space group	$P2_1/c$
a/Å	9.1806(9)
b/Å	14.5203(12)
c/Å	26.415(3)
α/°	90
β/°	94.737(4)
γ/°	90
Volume/Å^3	3509.2(6)
Z	4
ρ_{calc}g/cm^3	1.156
μ/mm^{-1}	0.643
F(000)	1244.0
Crystal size/mm^3	0.03 × 0.09 × 0.13
Radiation	MoKα (λ = 0.71073)
2Θ range for data collection/°	5.262 to 56.964
Index ranges	-12 ≤ h ≤ 12, -19 ≤ k ≤ 19, -35 ≤ l ≤ 35
Reflections collected	128225
Independent reflections	8647 [R_{int} = 0.1519, R_{sigma} = 0.2166]
Data/restraints/parameters	8647/0/362
Goodness-of-fit on F^2	0.909
Final R indexes [I>=2σ (I)]	R_1 = 0.0562, wR_2 = 0.1232
Final R indexes [all data]	R_1 = 0.1811, wR_2 = 0.1904
Largest diff. peak/hole / e Å^{-3}	0.45/-0.35
CCDC	2515600

Explanation of level B alerts in the crystal structure

- PLAT026_ALERT_3_B Ratio Observed / Unique Reflections (too) Low .. 38% Check
- PLAT230_ALERT_2_B Hirshfeld Test Diff for N0AA --C4. 8.0 s.u.
- PLAT241_ALERT_2_B High 'MainMol' Ueq as Compared to Neighbors of C20 Check

Response: These alerts are generated because of disorder in the structure, as the data is collected at room temperature.
https://doi.org/10.1039/D4DT02372B,https://doi.org/10.1039/C8SC05455J,https://doi.org/10.1021/acsami.1c07273.

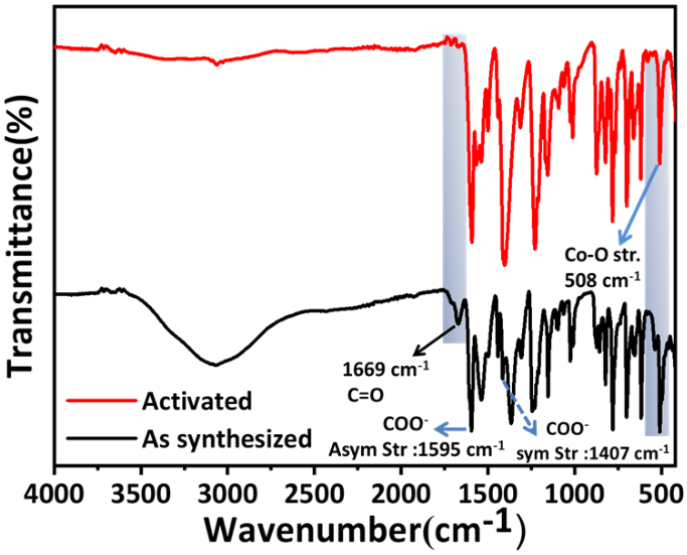

Fig. S3 FT-IR profile of as-synthesized and activated FCG-11, showing characteristic peaks.

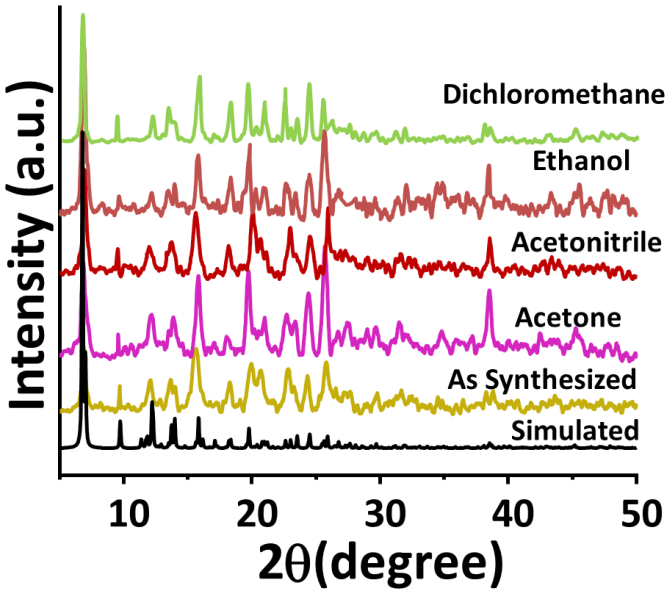

Fig. S4 PXRD pattern of FCG-11 in different organic solvents.

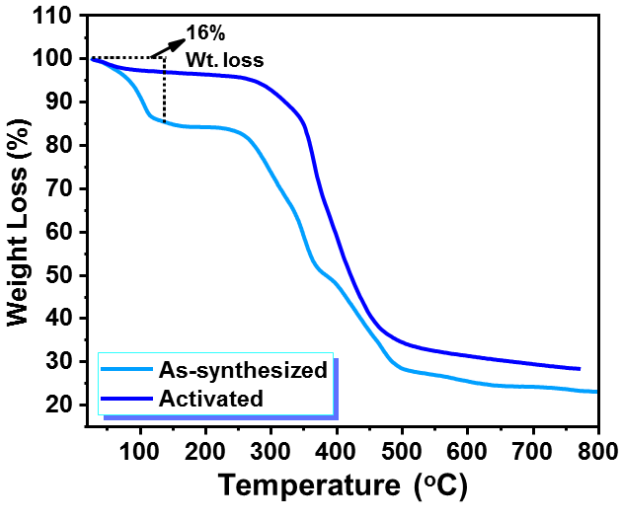

Fig. S5 Thermogravimetric analysis (TGA) plots of as-synthesized and activated FCG-11.

Section S5. Molecular formula determination of FCG-11 from PLATON and TGA analysis:

From the TGA plot of as-synthesized FCG-11, the observed mass loss is 16%.

From the PLATON Squeeze program, void electron count/formula unit comes out to be 67.

As DMF was used as a solvent during the synthesis of the MOF, the void space should be occupied by these lattice solvent molecules.

Now, the formula of the asymmetric unit is [Co(DPTz)(OBA)], and the mass of this asymmetric unit is 611.51.

Table S2. Number of electrons and molecular mass of guest molecules associated with FCG-11 for the determination of solvent composition and molecular formula.

	Dimethyl formamide (DMF)	Water
No. of electrons	40	10
mass	73	18

Considering the above-mentioned number of electrons, the best possible combination of solvent molecules for FCG-11 could be [Co(DPTz)(OBA)].1.5 DMF.1 H_2O.

The total number of electrons contributed by unlocated lattice molecules is 70, which is in close comparison with the PLATON result (electron count: 67) and thus validates the above formula.

The aforementioned combination was further cross-checked from the TGA analysis.

Mass loss due to lattice solvents is [(1.5 ×73) + (1 × 18)] = 127.5

Therefore, total mass of FCG-11 including lattice solvents is (611.51 + 127.5) = 739.01

So, mass loss due to DMF molecules is [(127.5/739.01) ×100] % = 17.25 %

Therefore, the total mass loss for the solvent is 17.25%, which is in good agreement with the TGA result (16%).

Hence, the chemical formula of FCG-11 is assigned as [Co(DPTz)(OBA)].1.5 DMF. 1 H_2O.

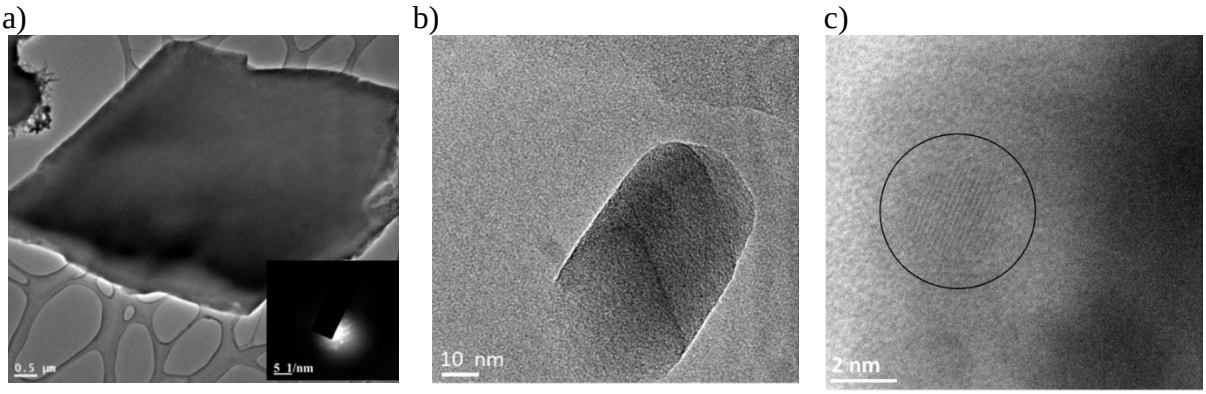

Fig. S6 (a) TEM image and corresponding SAED pattern (inset) of FCG-11. (b) HRTEM image of FCG-11, and (c) visible lattice fringes.

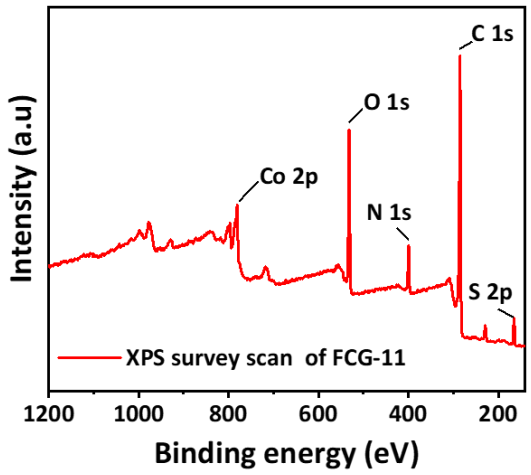

Fig. S7 XPS survey spectrum of FCG-11.

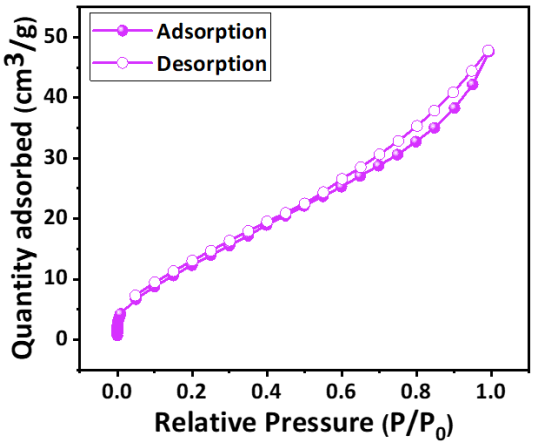

Fig. S8 N_2 adsorption isotherm of FCG-11 at 77K.

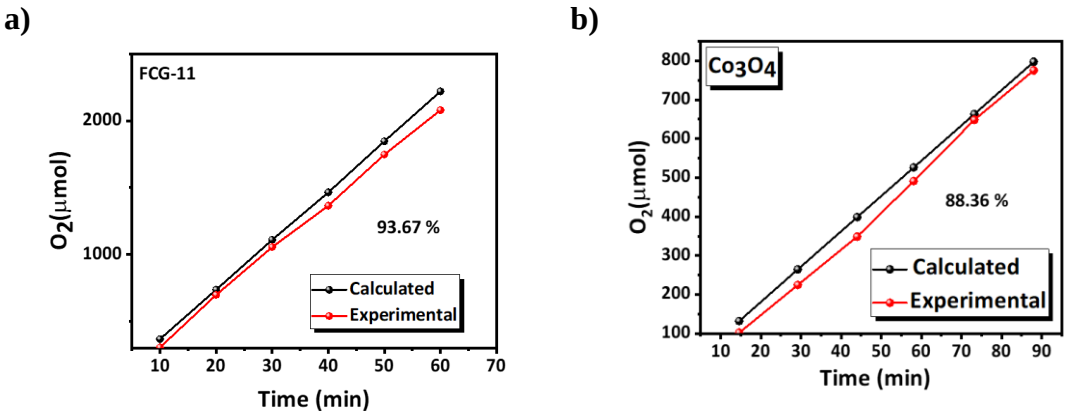

Fig. S9 (a) Comparison of calculated and experimentally determined O_2 evolution for FCG-11 during OER electrocatalysis. (b) Comparison of calculated and experimentally determined O_2 evolution for Co_3O_4 during OER electrocatalysis.

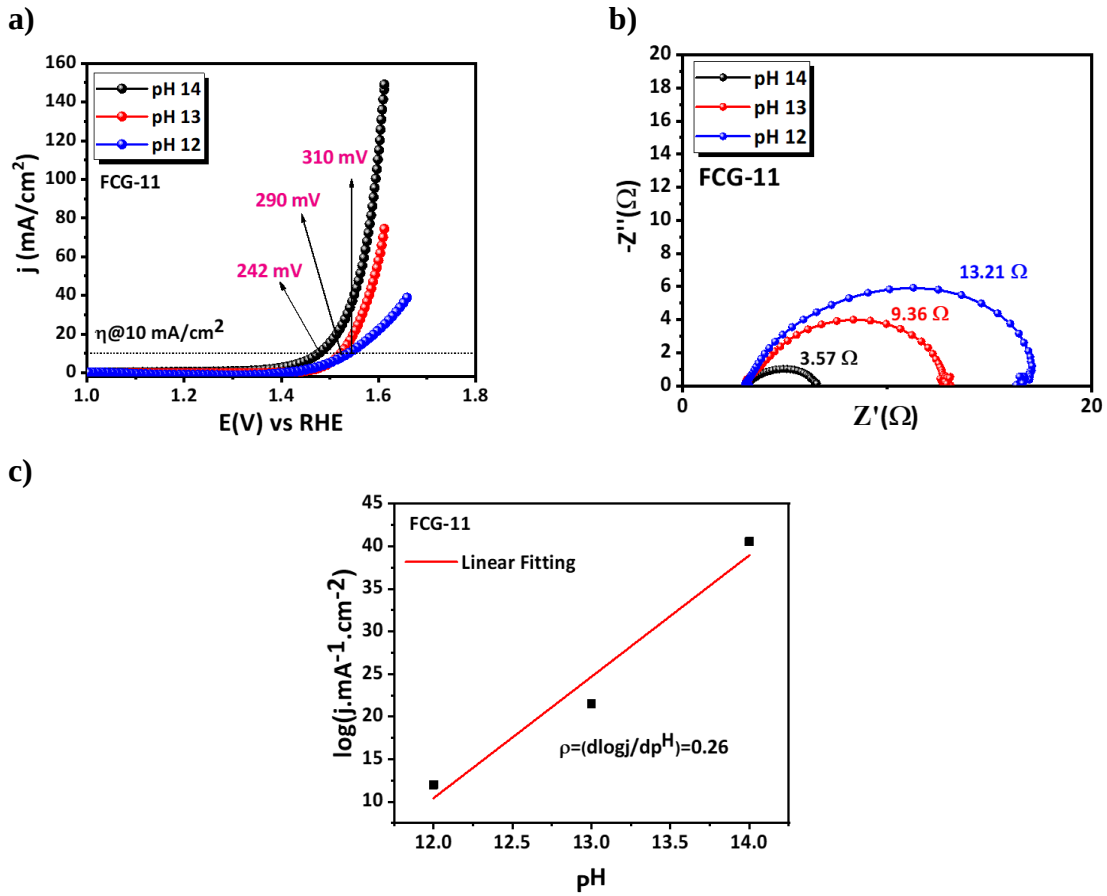

Fig. S10 (a) pH-dependent LSV measurement of FCG-11 catalyst towards OER at different pH. (b) Corresponding pH-dependent electrochemical impedance spectroscopy for FCG-11. (c) pH-dependent reaction order diagram for FCG-11.

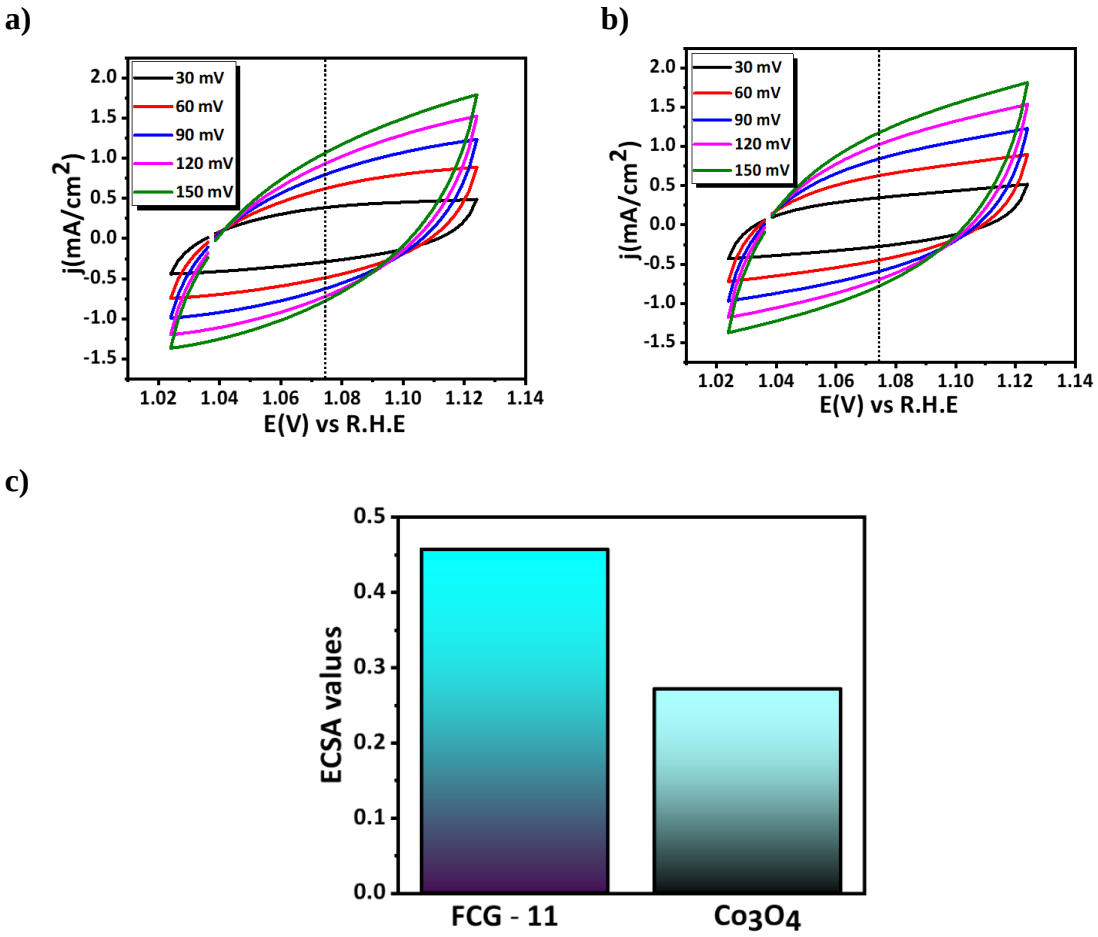

Fig. S11 (a-b) Cyclic voltammetry curves collected at varying scan rates within the non-faradaic region to evaluate the double-layer capacitance (C_{dl}). (c) ECSA values for FCG-11 and Co_3O_4.

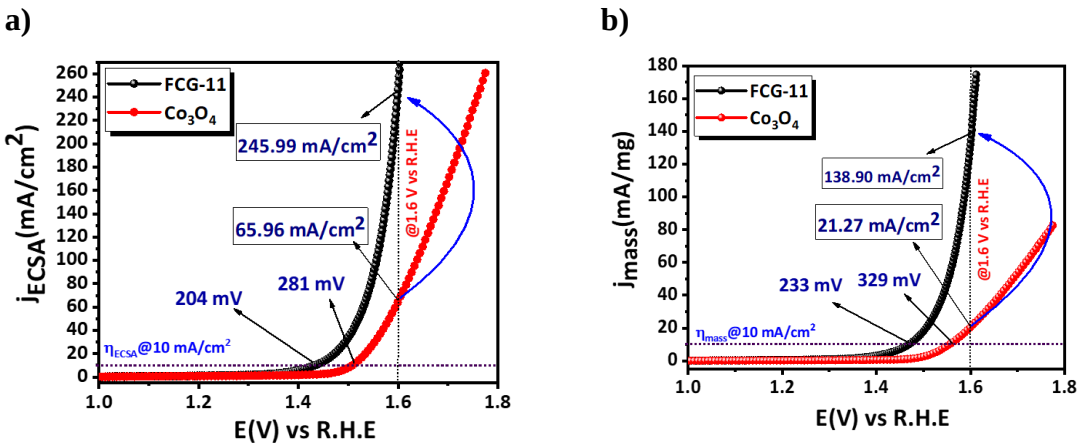

Fig. S12 (a) ECSA-normalized polarization curve. (b) mass-normalized polarization curve.

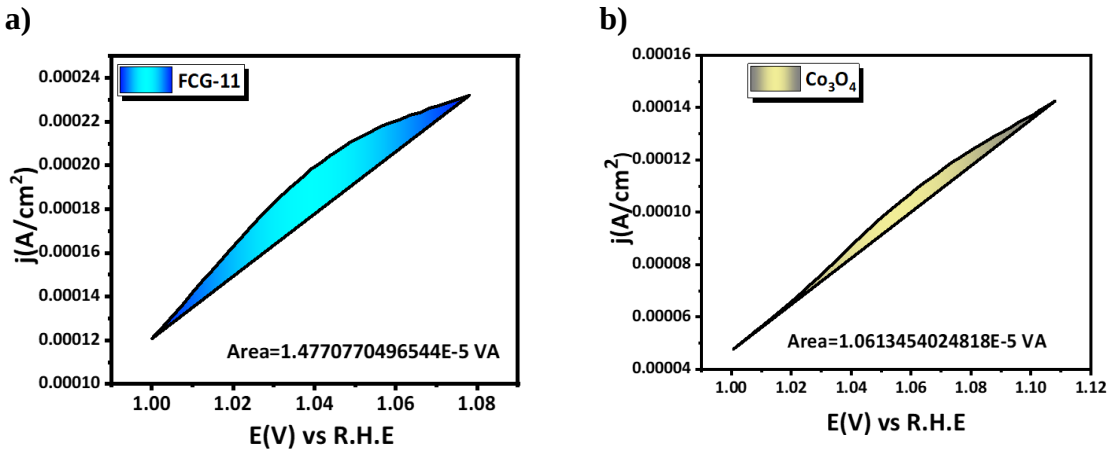

Fig. S13 Reduction surface area for (a) FCG-11 and (b) Co_3O_4.

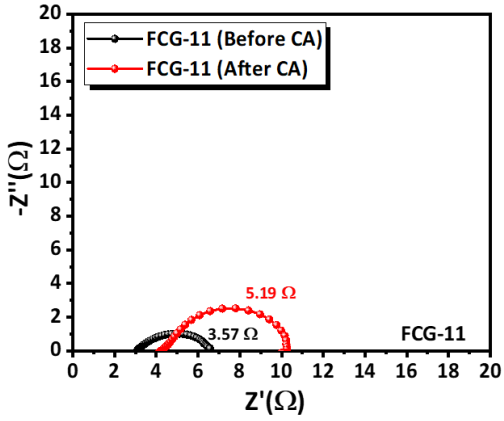

Fig. S14 Electrochemical impedance spectroscopy for FCG-11 after OER chronoamperometric study.

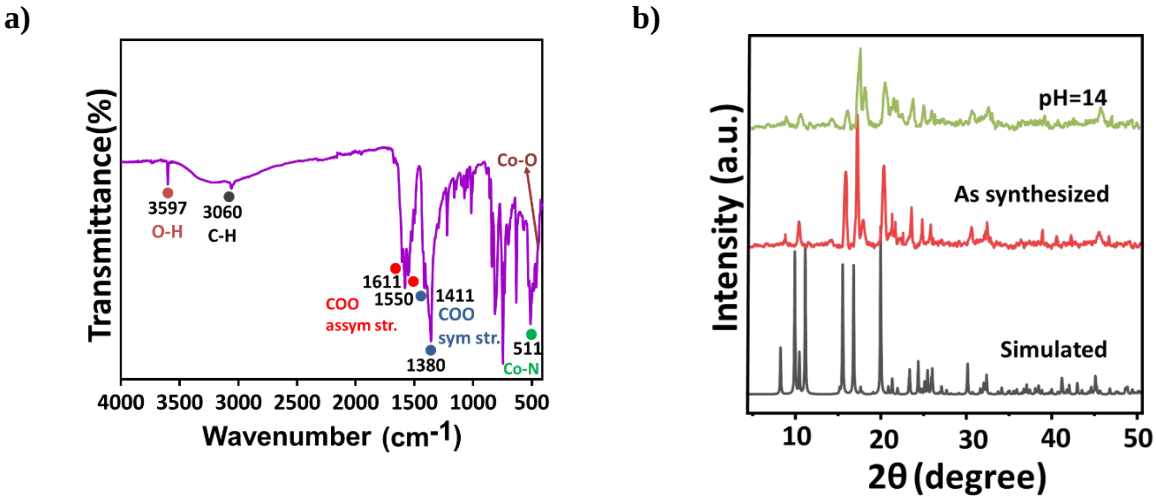

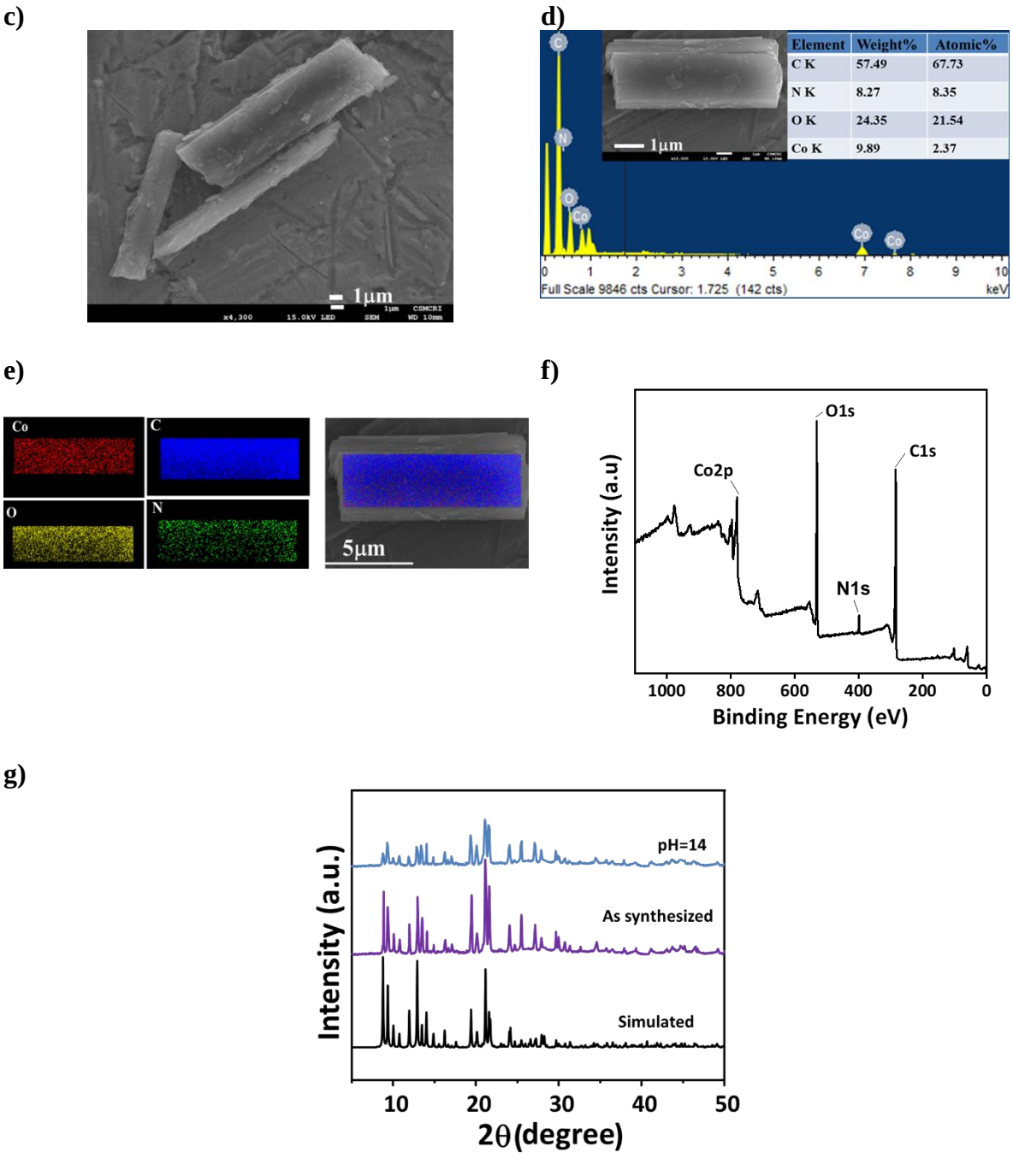

Fig. S15 Detailed characterization of MMOF using (a) FT-IR, and (b) PXRD, and (c) FE-SEM. (d) EDX spectrum and (e) elemental mapping analysis of MMOF. (f) XPS survey spectrum of MMOF. (g) The PXRD pattern of simulated, as-synthesized, and at pH: 14 for FCG-10.

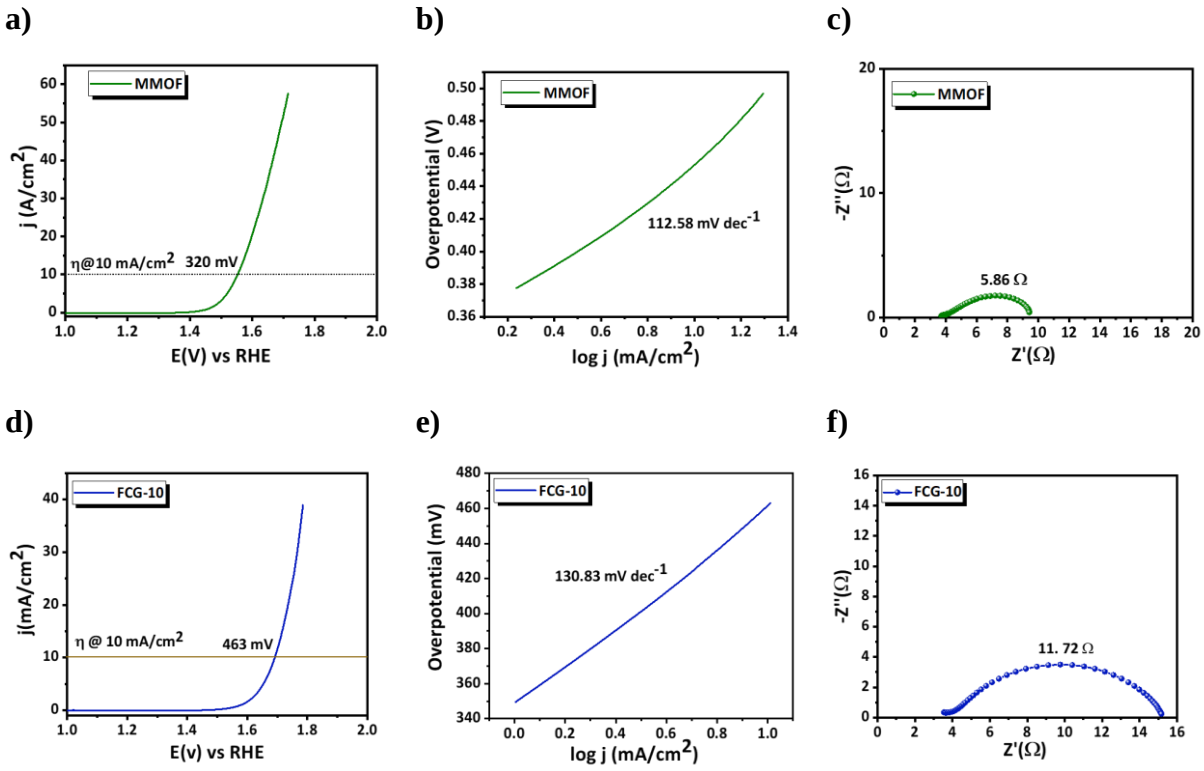

Fig. S16 Electrocatalytic OER performance of MMOF and FCG-10 in alkaline medium (1 M KOH): (a-c) LSV polarization curves, Tafel slope and EIS of MMOF; (d-f) LSV polarization curves, Tafel slope and EIS of FCG-10.

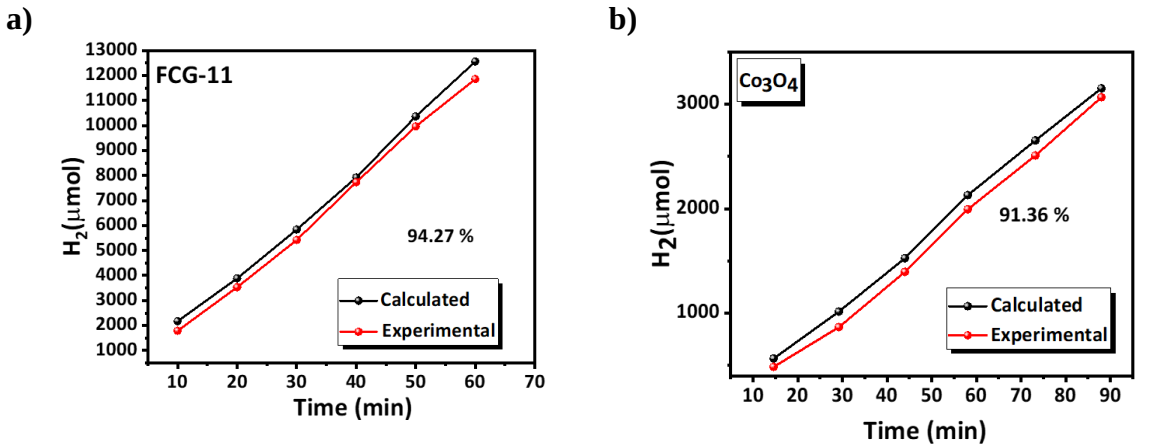

Fig. S17 (a) Calculated and experimental amount of H_2 evolution for FCG-11 during HER process. (b) Calculated and experimental amount of H_2 evolution for Co_3O_4 during HER process.

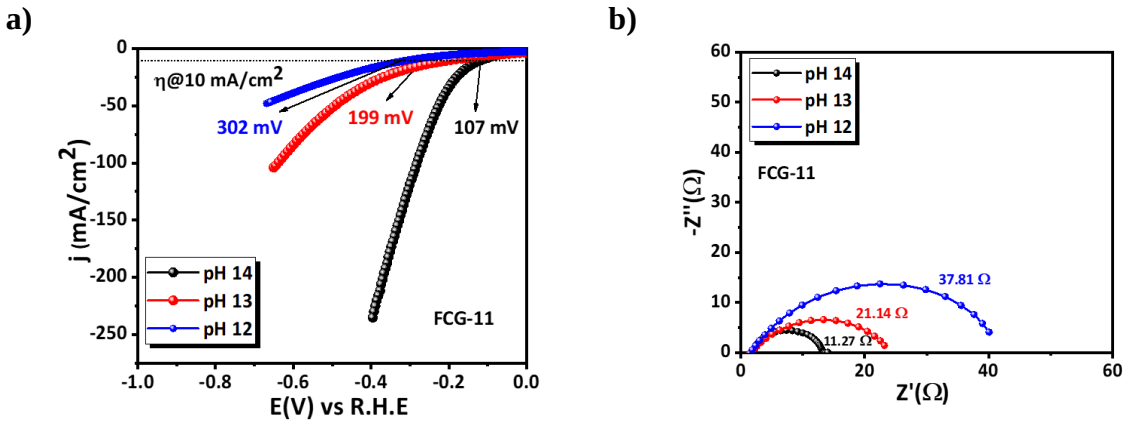

Fig. S18 (a) pH-dependent LSV measurement of FCG-11 catalyst towards HER at different pH environments. (b) Corresponding pH-dependent electrochemical impedance spectroscopy for FCG-11.

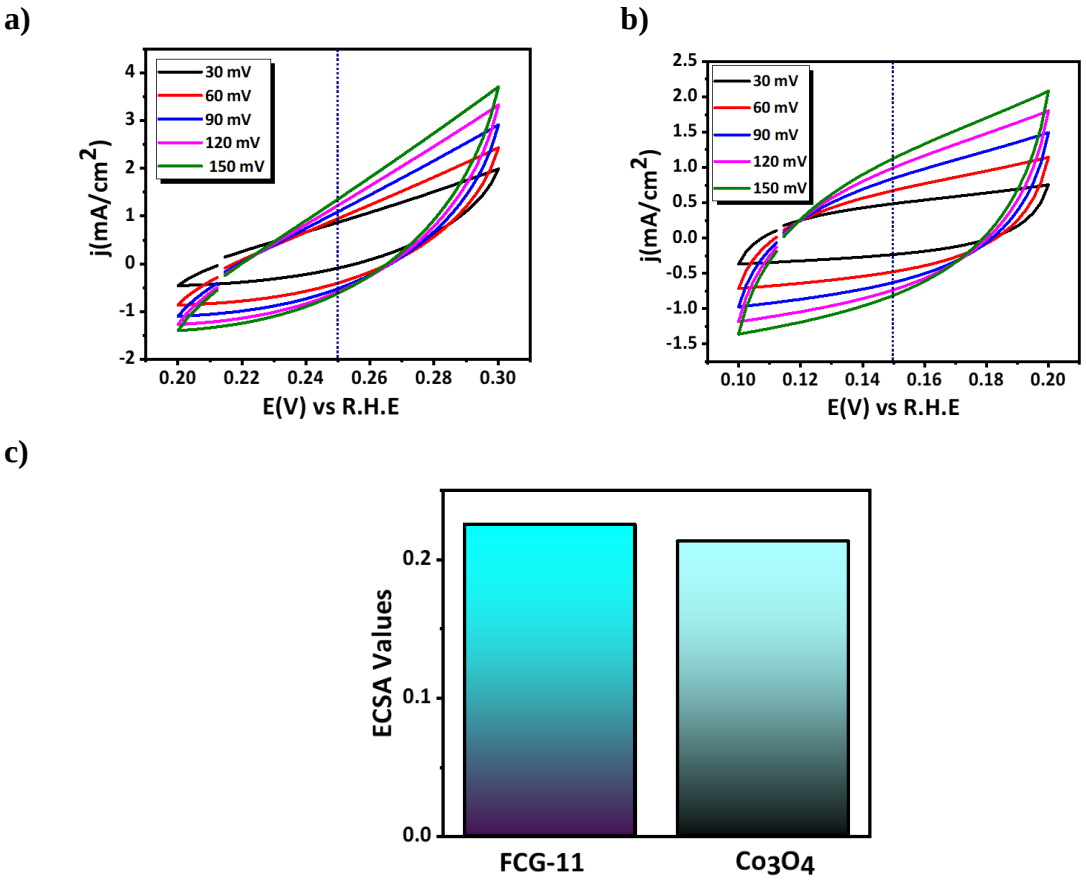

Fig. S19 (a-b) scan rate-dependent CV curves obtained for calculating the C_{dl} value in the non-faradaic region. (c) Calculated ECSA values of FCG-11 and Co_3O_4.

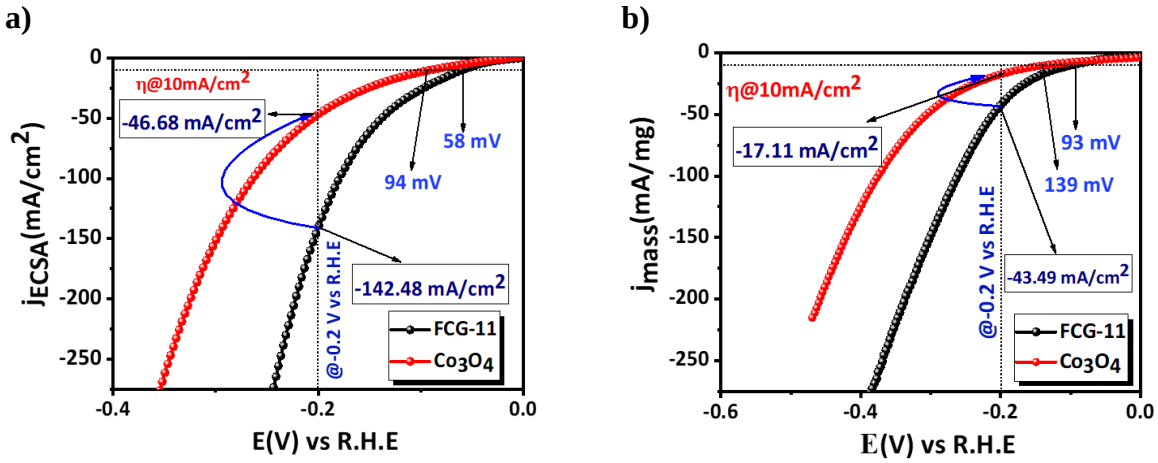

Fig. S20 (a) ECSA-normalized polarization curve. (b) Mass-normalized polarization curve for FCG-11 during HER.

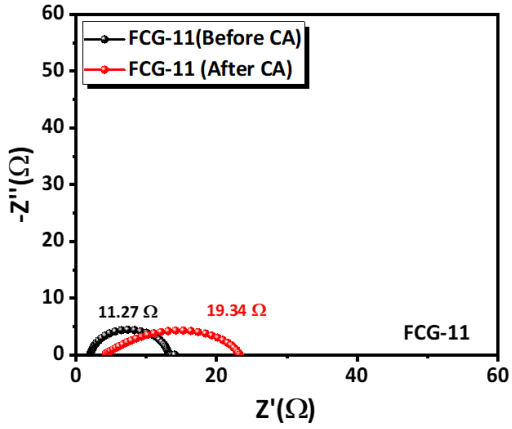

Fig. S21 Electrochemical impedance spectroscopy for FCG-11 after chronoamperometric study for HER.

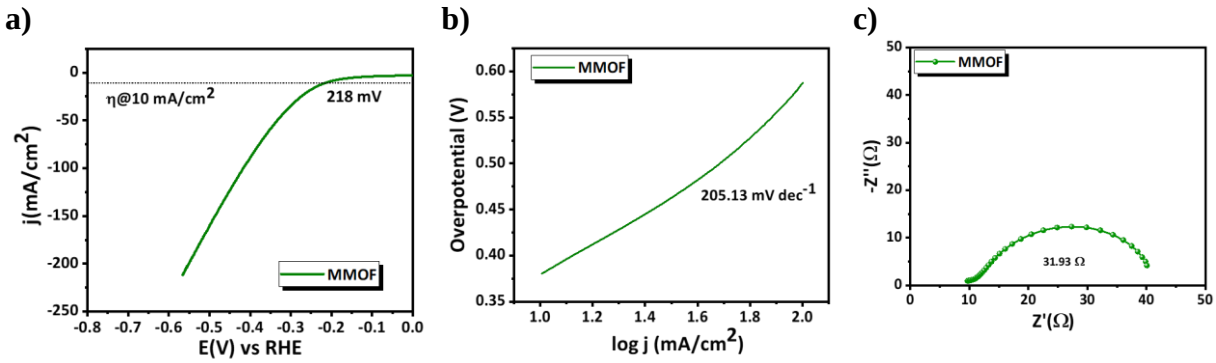

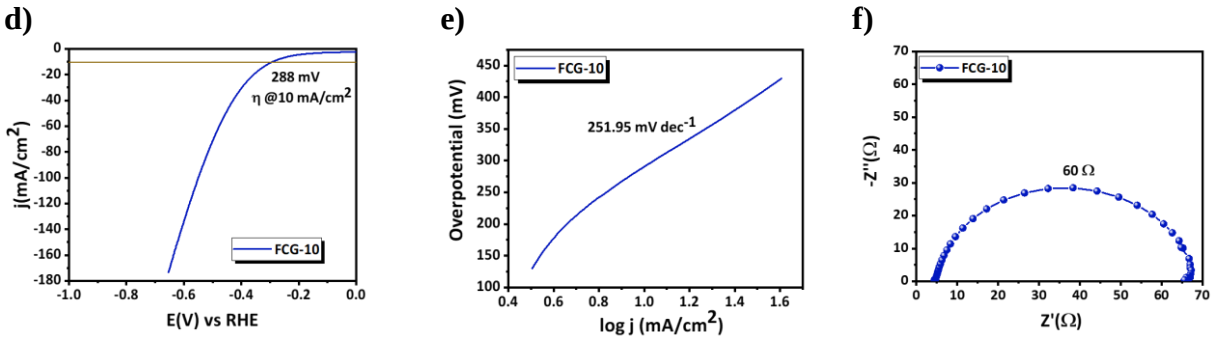

Fig. S22 Electrocatalytic HER performance of MMOF and FCG-10 in alkaline medium. (a-c) LSV polarization curves, Tafel slope, and EIS of MMOF; (d-f) LSV polarization curves, Tafel slope and EIS of FCG-10.

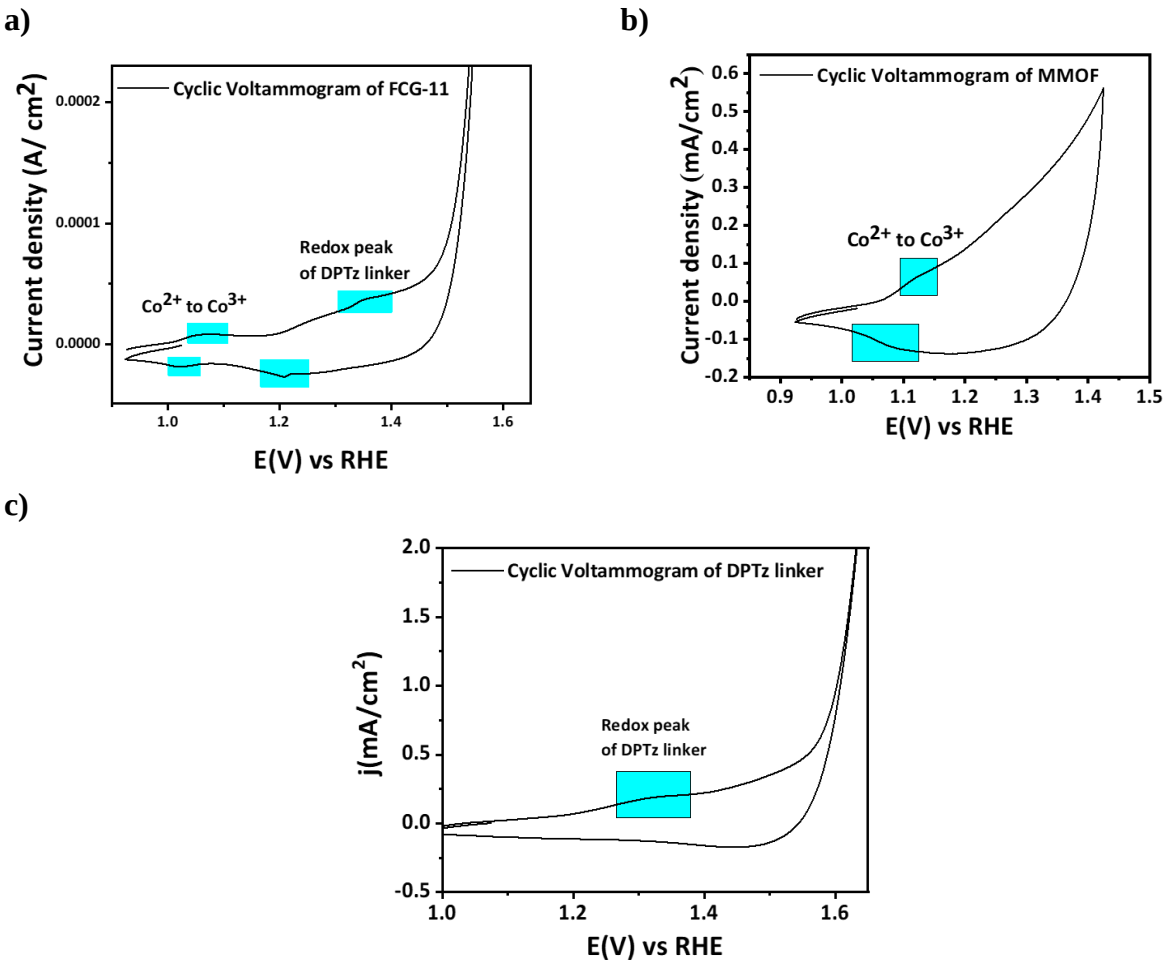

Fig. S23 (a) Cyclic voltammogram of FCG-11. (b) Cyclic voltammogram of MMOF. (c) Cyclic voltammogram of free DPTz linker.

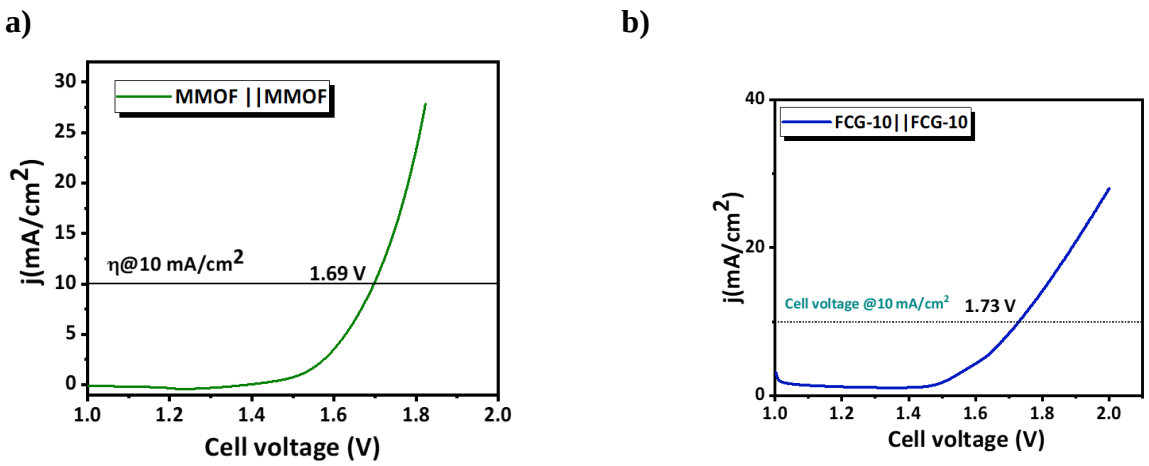

Fig. S24 (a) LSV polarization curve recorded for evaluating the total water splitting performance of the MMOF catalyst. (b) LSV polarization curve recorded for evaluating the total water splitting performance of the FCG-10 catalyst.

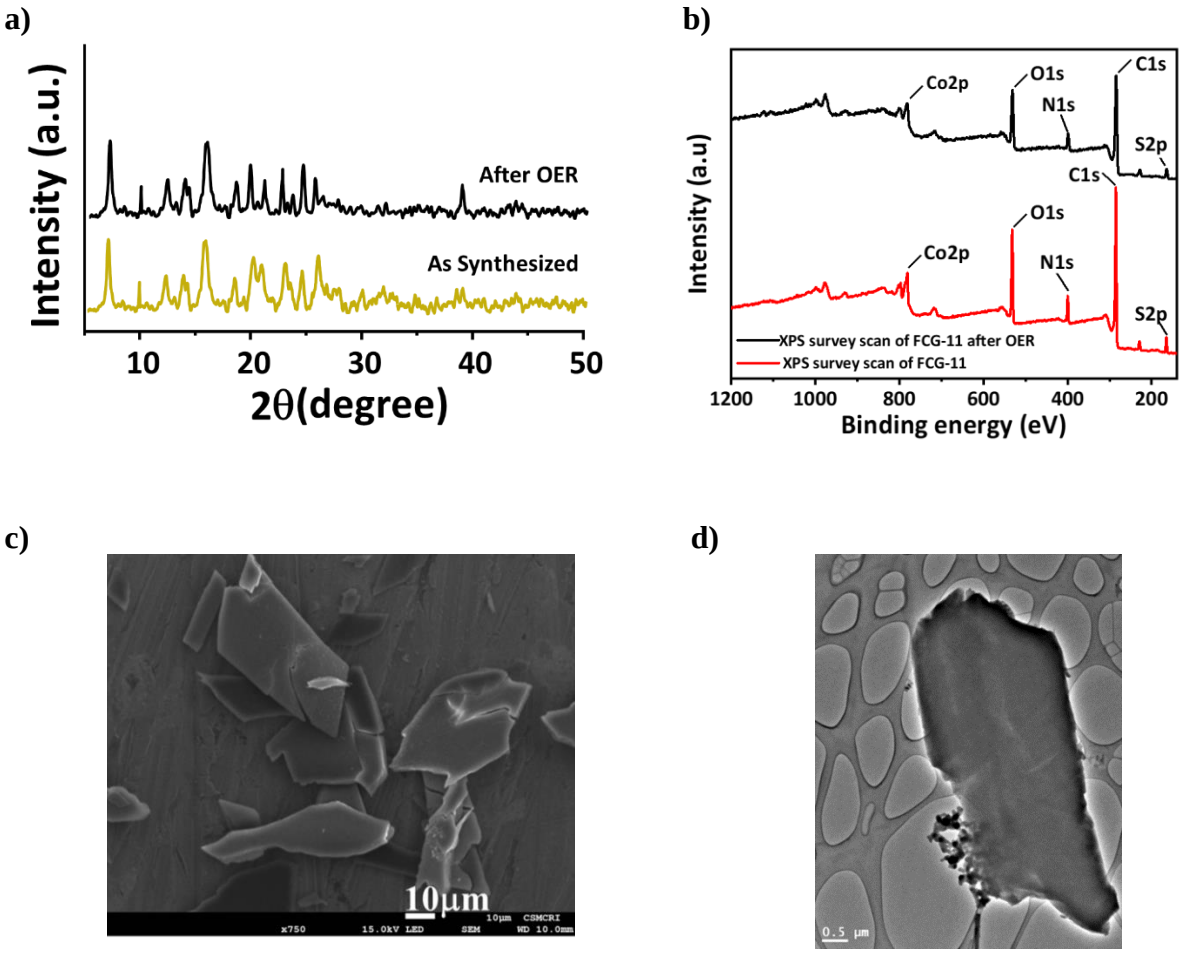

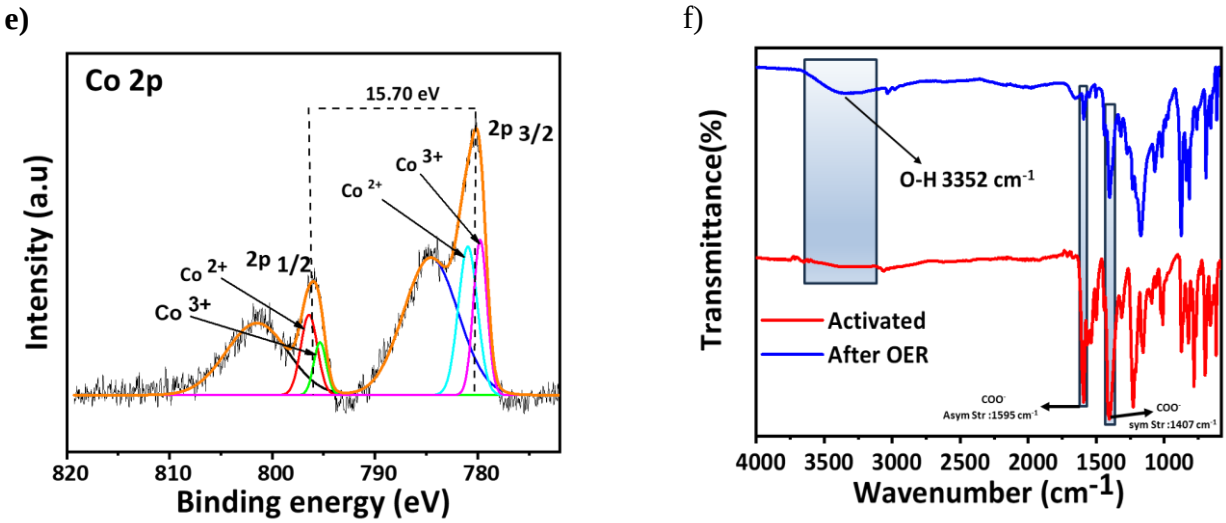

Fig. S25 (a) PXRD pattern and (b) XPS survey spectrum of FCG-11 before and after OER. (c) FE-SEM image of FCG-11 after OER. (d) TEM image of FCG-11 after OER. (e) Post OER Co 2p XPS spectrum of FCG-11 electrocatalyst. f) FT-IR spectra of FCG-11 before and after OER.

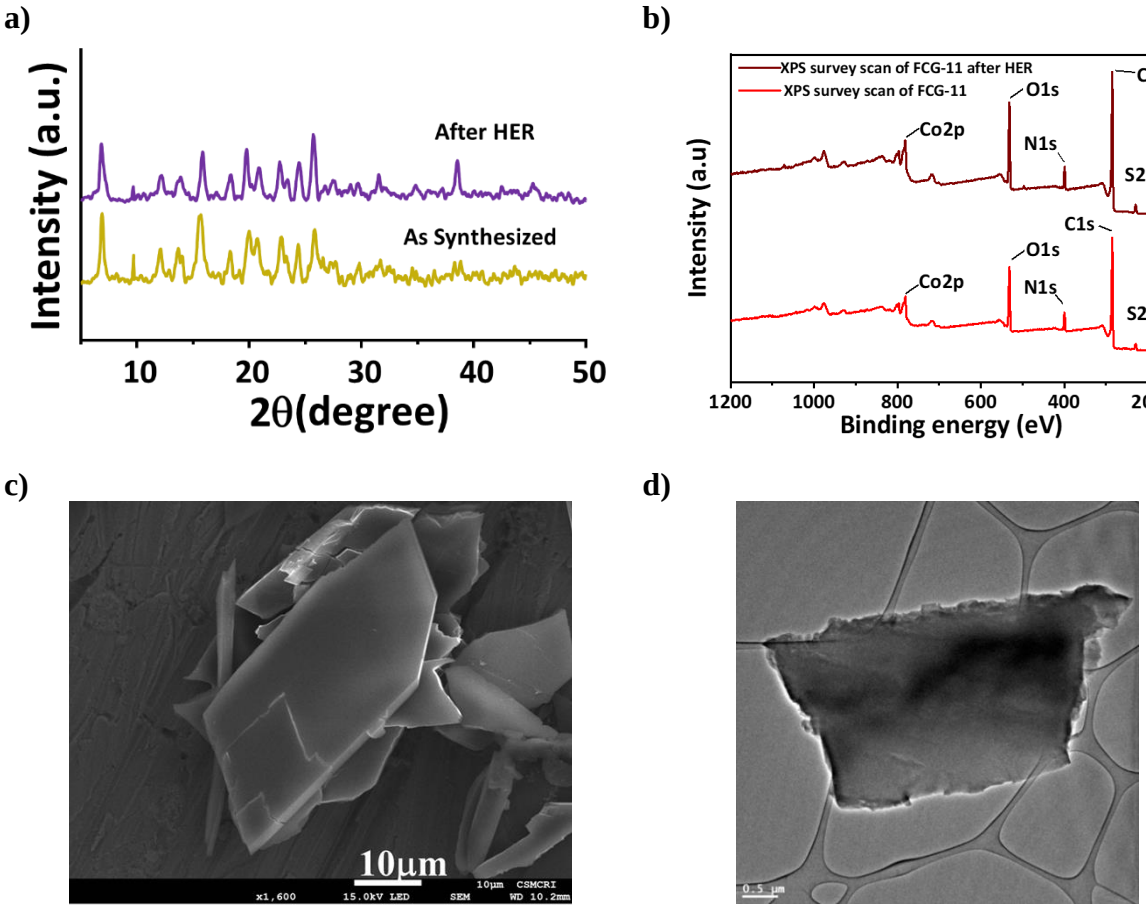

Fig. S26 (a) PXRD pattern and (b) XPS survey spectrum of FCG-11 before and after HER. (c) FE-SEM image of FCG-11 after HER. (d) TEM images of FCG-11 after HER.

a) **b)**

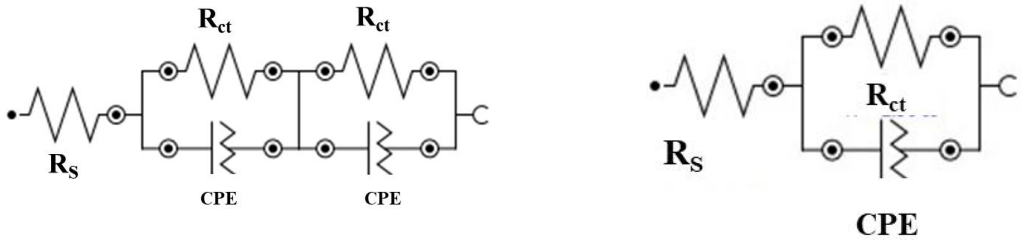

Fig. S27 Electronic equivalent circuit (EEC) for modelling EIS data for (a) OER and (b) HER by FCG-11 catalyst.

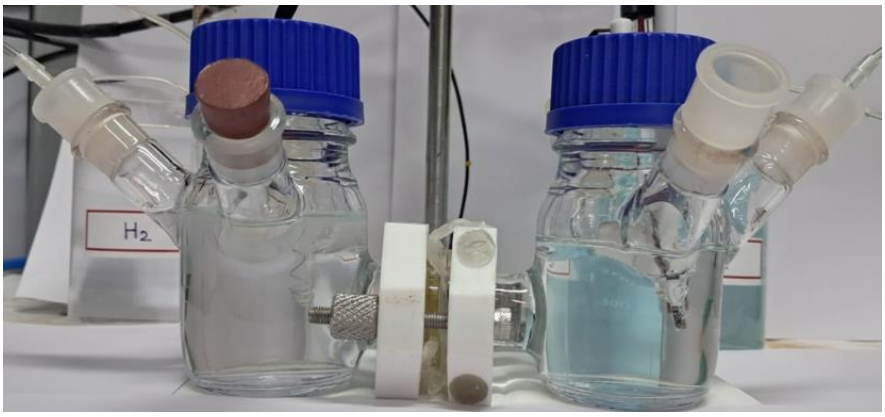

Fig. S28 Water-gas displacement setup used for the Faradic efficiency determination of the FCG-11.

Section S6. Computational methodology

All the theoretical calculations of all MOF geometries and its energy estimation were performed by 'Becke three-parameter and Lee Yang Par' functional (B3LYP)[7, 8] comprising with the 6-31+G(d) basis set.[9] All of this calculation carried out using the Gaussian09 software package.[10] The Co atom was treated using the LANL2DZ basis set along with an effective core potential.[11] Frequency calculations were also performed at the B3LYP/6-+31G(d) level of theory to ensure the stability of these optimized geometries. The absence of imaginary frequencies confirmed that all optimized geometries are in true minima. Furthermore, solvent-phase calculations were performed using the Self-Consistent Reaction Field (SCRF) method within the Polarizable Continuum Model (PCM, water, $\varepsilon = 78.3553$).[12] To evaluate the reaction free energies, thermal corrections and zero-point vibrational energy (ZPVE) were also incorporated into the total electronic energies.

The adsorption free energies (ΔG) were calculated using the following equation developed by Norskov et al.[13] as follows:

$$\Delta G = \Delta E + \Delta ZPE - T\Delta S - neU \quad \text{.....(E13)}$$

Here the ΔE represent the total energy difference between the initial and final states, where ΔZPE signify the change in zero-point energy (ZPE) at temperature T, and ΔS denotes the entropy of the reaction. In neU where the n represents the number of electron transfer in each elementary reaction step. The electrochemical potential was referenced to the reversible hydrogen electrode (RHE) using the computational hydrogen electrode (CHE) model.

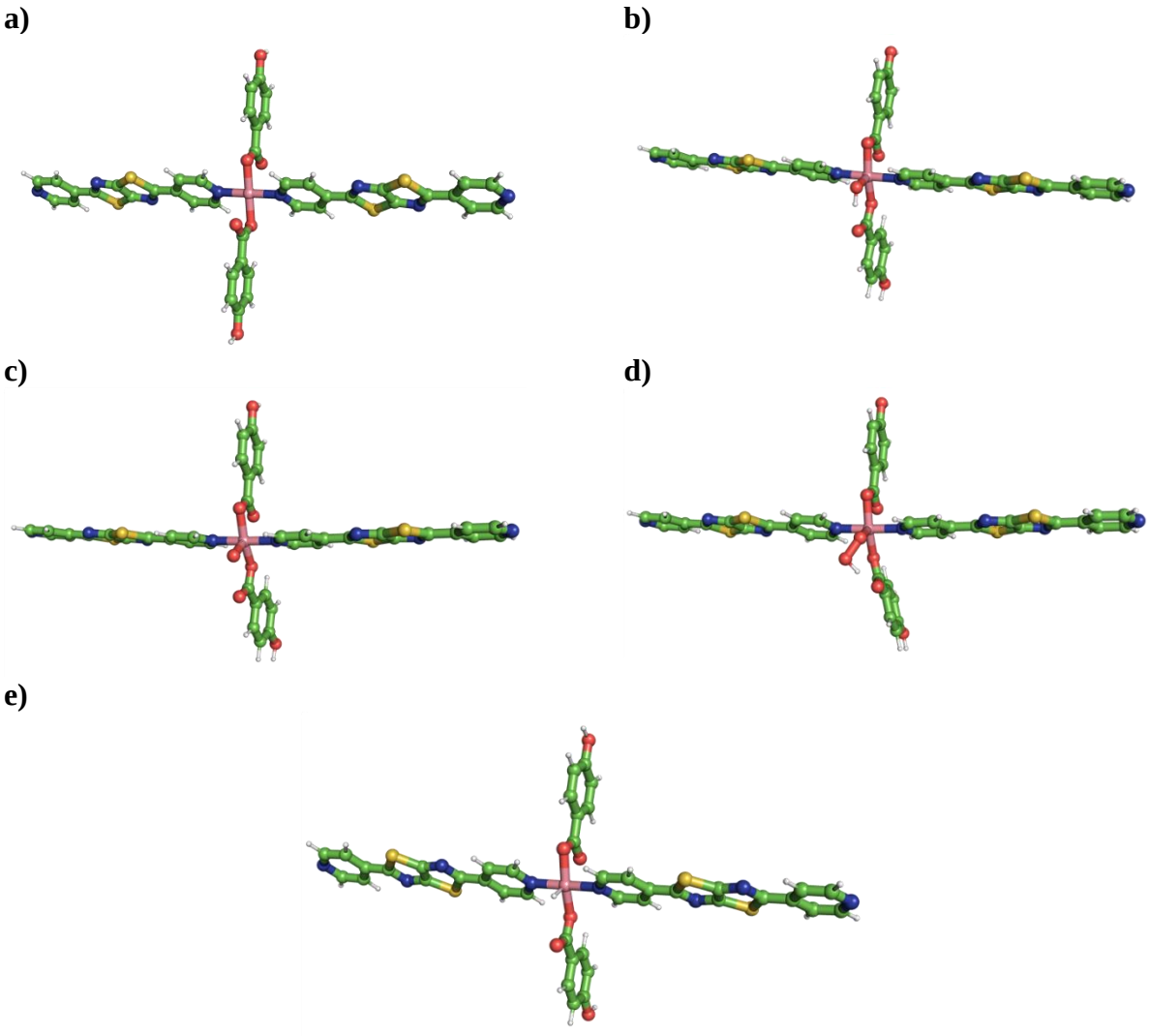

Fig. S29 Optimized structures of a) FCG-11 catalyst, and b) *OH, c) *O, d) *OOH, and e) *H adsorbed FCG-11 catalyst.

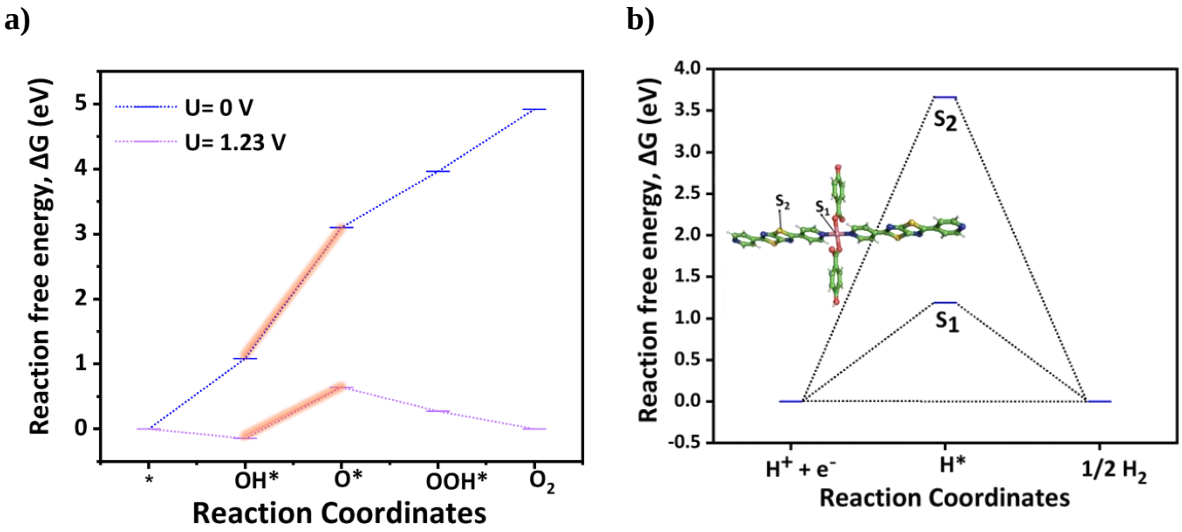

Fig. S30 a) Reaction free energy profile diagram of FCG-11 at U=0 V and U=1.23 V, respectively, derived from the adsorption at the metal centre of O*, OH*, and OOH* intermediate for OER and b) reaction free energy profile diagram of the FCG-11 catalyst for HER, illustrating hydrogen adsorption at different active sites**.**

Table S3. Comparison of the electrocatalytic OER performance of FCG-11 catalyst relative to contemporary reported materials.

Entry	Material	Overpotential (mV)	Tafel Slope (mV dec^{-1})	TOF (S^{-1})	Reference
1.	UTSA-16	408	77	-	[14]
2.	IITG-7a	351	93	13.3566	[15]
3.	CSMCRI-10	396	102	0.03	[16]
4.	HFC Co_3O_4	400	70	1.67×10^{-2}	[17]
5.	CoCu-MOF NBs	271	63.5	0.326	[18]
6.	CoS_x@MoS_2	347	147	-	[19]
7.	MOF-1	420	126.13	0.1	[20]
8.	Co:Fe	453	63	0.088	[21]
9.	$Co_2(OH)_2$BDC nanosheets	273	74	0.23	[22]
10.	CoCe-MOF/CP	267	96.1	-	[23]

11.	Co_3Cu-Ni_2MOFs	288	87	0.05	[24]
12.	Co-MOF-C	342	119	0.045	[25]
13.	Co_4Fe_6-MOF	241	30.1	1.04	[26]
14.	FCG-2	375	78	1.74	[27]
15.	Co-BTC	370	89.1	1.23	[28]
16.	Ek-a	413	77	0.004	[29]
17.	MOF-Fe/Co(1:2)	238	52	-	[30]
18.	Co_2(dobpdc)-III	278	92.8	-	[31]
19.	Co-MOF	420	90	-	[32]
20.	**FCG-11**	**242**	**90.82**	**3.42**	**This work**
21.	**MMOF**	**320**	**112.58**	**-**	**This work**
22.	**FCG-10**	**463**	**130.83**	**-**	**This work**

Table S4. Comparison of the electrocatalytic HER performance of FCG-11 catalyst relative to contemporary reported materials.

Entry	Material	Overpotential (mV)	Tafel Slope (mV dec^{-1})	TOF (S^{-1})	Reference
1.	Co–BTC	437	115.1	2.42	[28]
2.	Co-MOF	222	157	-	[33]
3.	Co-MOF 1 Co-MOF 2 Co-MOF 3 Co-MOF 4	344 279 215 185	159.5 134.6 128.1 123.7	-	[34]
4.	$\{[Co_{2.5}(L)]\cdot 5H_2O\}_n$ $0.5\{[Cu(L)]\cdot 2H_2O\}_n$	567 585	183 195	-	[25]
5.	Co/NBC-900	117	146	-	[35]
6.	Co-MOF	170	89	-	[32]
7.	Co-NC/CF	157	109	-	[36]
8.	Co-P FeCo-P	167 131	123.24 89.90	0.026 0.134	[37]
9.	Co-MOFs Co-MOFs-800	128 112	129 127	0.32 0.38	[38]
10.	Co-BDC Co-BDC/MoS_2	529 248	111 86	- -	[39]
11.	Fe-Co-O/Co@NCmNS/NF Fe-Co-	112 141	96 118	- -	[40]

	O/Co@NC/NF				
12.	CC/MOF	186.10	172.16	-	[41]
13.	B-CoO/Co@NC/NF (Ar) B-CoO/Co@NC/NF (10% H_2) B-CoO/Co@NC/NF (50% H_2)	264 196 251	134.2 132.7 134.8	- - -	[42]
14.	FeCo-P	131	89.90	0.134	[37]
15.	**FCG-11**	**107**	**70.22**	**13.18**	**This work**
16.	**MMOF**	**218**	**205.13**	**-**	**This work**
17.	**FCG-10**	**288**	**251.95**	**-**	**This work**

Table S5. Comparison of the electrocatalytic TWS performance of FCG-11 catalyst relative to reported contemporary materials.

Entry	Material	Cell voltage(V)@Current density (10 mA cm^{-2})	Reference
1.	Co–BTC/CC	2.03	[28]
2.	Co-MOF 1 Co-MOF 2 Co-MOF 3 Co-MOF 4	1.88 1.80 1.71 1.56	[34]
3.	Fe-CoP NFs	1.65	[43]
4.	Co-P@PC-750	1.60	[44]
5.	$Co_{0.45}Fe_{0.45}Ni_{0.9}$–MOF/NF	1.59	[45]
6.	Co-NC@Mo_2C	1.685	[46]
7.	Co-P/NC	1.81	[47]
8.	NBU-4 /NF@CoOOH	1.65	[48]
9.	NiCo-LDH@NH_2-UiO-66	1.65	[49]
10.	$(Fe_{0.1}Ni_{0.9})_2P(O)$/NF	1.50	[50]
11.	NiCoP	1.64	[51]
12.	**FCG-11**	**1.58**	**This work**
13.	**MMOF**	**1.69**	**This work**
14.	**FCG-10**	**1.73**	**This work**

Table S6. The Cartesian coordinates of the optimized FCG-11 and complex systems at the B3LYP/6-31+G(d) level of theory in the aqueous phase. The corresponding electronic energies are given in Hartree.

FCG-11 **E = -4243.541660**				**FCG-11+ O*** **E = -4318.672019**			
Co	-0.00001900	0.00005400	-0.00008900	Co	0.02033600	0.04847400	-0.59775100
S	9.75567100	0.58294600	1.43682100	S	9.76361600	-0.85768000	-1.78160800
S	7.17802700	-0.75022800	-1.52209500	S	7.16005200	0.53590400	1.12636600
N	1.98369700	-0.05912900	-0.04241600	N	1.99573000	0.04766900	-0.50195600
N	6.98542200	0.32294600	0.86953100	N	6.99051600	-0.51769300	-1.27548700
N	9.94707400	-0.48972600	-0.95595900	N	9.93215100	0.19604700	0.62161000
N	14.96803700	-0.06017300	-0.05434200	N	14.95737400	-0.37062000	-0.17552500
C	2.63424500	-0.61429800	-1.08242300	C	2.62439900	0.51642100	0.59015800
H	2.01490000	-1.03748300	-1.86439300	H	1.99326000	0.91002500	1.37691600
C	4.02068000	-0.65997900	-1.16202900	C	4.00855800	0.50882000	0.70828300
H	4.47598600	-1.11999700	-2.03297100	H	4.45339500	0.90749600	1.61400300
C	4.79099100	-0.11991800	-0.11958000	C	4.78884600	-0.00782100	-0.33869300
C	6.25710100	-0.12914100	-0.13198200	C	6.25352000	-0.04965200	-0.28766500
C	8.29802800	0.19184200	0.57424700	C	8.29892500	-0.42901800	-0.94938100
C	8.63381500	-0.36101300	-0.65818100	C	8.62273800	0.10658400	0.29417600
C	10.67629800	-0.03673400	0.04382700	C	10.66999500	-0.27087200	-0.36541400
C	12.14447000	-0.03537400	0.03029400	C	12.13693200	-0.31380100	-0.32040700
C	12.91027300	0.49208700	1.08210200	C	12.91123800	-0.82087400	-1.37597100
H	12.44967700	0.93045900	1.96234100	H	12.45868200	-1.20966700	-2.28326000
C	14.30147400	0.45479600	0.99087300	C	14.30056100	-0.82594200	-1.25406300
H	14.90756300	0.86001100	1.79786300	H	14.91327700	-1.21568200	-2.06365700
C	14.22957200	-0.56283300	-1.05869400	C	14.21079200	0.11348700	0.83190100
H	14.78080200	-0.97730200	-1.89978100	H	14.75425400	0.47941200	1.70011300
C	12.83654200	-0.57580400	-1.06746600	C	12.81871800	0.16480600	0.81187600
H	12.29527900	-0.99683300	-1.90710100	H	12.27051400	0.56757700	1.65594300
C	4.10291200	0.44789200	0.96724300	C	4.11466200	-0.49703400	-1.47162600
H	4.64636300	0.87701700	1.80051900	H	4.66759900	-0.90727400	-2.30800900
C	2.71508800	0.46274700	0.96318700	C	2.72865600	-0.45032000	-1.51479700
H	2.15707000	0.91031500	1.77721900	H	2.17306600	-0.80241300	-2.37470300
O	0.07160100	1.84341800	0.67222000	O	0.04131900	-1.90977700	-0.75944700
O	0.02710700	1.95566500	-1.54378100	O	-0.03030000	-0.97348100	1.20763400
O	-0.07161800	-1.84330300	-0.67240700	O	-0.01223500	1.80107500	0.10879100
N	-1.98374200	0.05922300	0.04227600	N	-1.95714700	0.01672100	-0.63109400
S	-7.17803000	0.75043100	1.52206000	S	-7.15837800	-0.80641200	-1.97584600
S	-9.75576600	-0.58322300	-1.43655900	S	-9.68765400	0.39483900	1.07975700
N	-14.96808400	0.05990800	0.05477400	N	-14.91512900	-0.46210400	-0.24170100
N	-9.94709400	0.48977100	0.95608300	N	-9.91472900	-0.66153400	-1.31749800
N	-6.98549900	-0.32306900	-0.86942500	N	-6.92951400	0.24938000	0.42033300
C	-14.30155600	-0.45500500	-0.99049000	C	-14.23293700	0.00743700	0.81473600
H	-14.90767000	-0.86021400	-1.79746400	H	-14.82539600	0.32576200	1.66938800
C	-12.91035800	-0.49224300	-1.08179000	C	-12.84216700	0.10061900	0.86119500
H	-12.44979100	-0.93056100	-1.96207100	H	-12.36791300	0.49111200	1.75657600
C	-12.14452100	0.03521100	-0.03000400	C	-12.09425500	-0.31506000	-0.25176400
C	-10.67635000	0.03662200	-0.04360900	C	-10.62779500	-0.25158600	-0.28791300
C	-8.63384400	0.36105600	0.65826400	C	-8.59874200	-0.48116200	-1.06202200
C	-8.29809500	-0.19195700	-0.57410400	C	-8.24482400	0.07179800	0.16560800
C	-6.25714700	0.12917300	0.13199600	C	-6.21759100	-0.16356000	-0.60957000
C	-4.79103700	0.11997700	0.11953700	C	-4.75281900	-0.10664800	-0.63896500
C	-4.02069600	0.66020200	1.16187700	C	-4.00005300	-0.55348000	-1.73705100
H	-4.47597600	1.12033800	2.03277200	H	-4.46911800	-0.96303500	-2.62552400
C	-2.63426300	0.61453500	1.08222600	C	-2.61385000	-0.47487100	-1.69539900
H	-2.01489500	1.03784300	1.86411000	H	-1.99849700	-0.79559600	-2.52623600
C	-2.71516400	-0.46281200	-0.96322300	C	-2.66329600	0.45052600	0.43023800
H	-2.15717000	-0.91049100	-1.77720900	H	-2.08893800	0.84010000	1.26137800
C	-4.10298900	-0.44797900	-0.96723000	C	-4.04981400	0.40861600	0.46449000
H	-4.64646400	-0.87723300	-1.80042300	H	-4.57971100	0.76966300	1.33765500
C	-12.83655700	0.57558200	1.06780700	C	-12.80271100	-0.80821400	-1.36124300

H	-12.29526600	0.99660000	1.90743000
C	-14.22958700	0.56256300	1.05910500
H	-14.78079000	0.97698600	1.90023200
O	-0.02706700	-1.95558500	1.54359200
C	-0.07344500	-2.52844100	0.42556900
C	-0.13418700	-4.01748900	0.31958200
C	-0.11124300	-4.80515600	1.48101600
H	-0.04806400	-4.31784500	2.44869600
C	-0.16737900	-6.19580000	1.40662500
H	-0.14745600	-6.79516100	2.31420200
C	-0.24987700	-6.81824100	0.15286100
C	-0.27504500	-6.04657200	-1.01749300
H	-0.34028900	-6.54396100	-1.98084900
C	-0.21678100	-4.65838800	-0.92871500
H	-0.23701100	-4.05926500	-1.83319100
O	-0.30867400	-8.17684900	0.00845100
O	0.30891400	8.17694500	-0.00874300
C	0.25006500	6.81833700	-0.15313000
C	0.27518400	6.04668700	1.01723800
H	0.34043200	6.54409100	1.98058700
C	0.21686600	4.65850400	0.92848300
H	0.23705700	4.05939600	1.83297100
C	0.13426600	4.01758700	-0.31980400
C	0.07346300	2.52853900	-0.42576500
C	0.11137200	4.80523300	-1.48125200
H	0.04819000	4.31790800	-2.44892400
C	0.16756300	6.19587700	-1.40688400
H	0.14767700	6.79522300	-2.31447200
H	0.28593400	8.61094800	-0.87823300
H	-0.28566400	-8.61086700	0.87793200

FCG-11+ OH*
E = -4319.348109

Co	0.02050900	-0.02615900	-0.54886700
S	9.75632600	-0.73972700	-1.88517800
S	7.16995400	0.50185400	1.10569400
N	1.99268300	-0.00360300	-0.47213400
N	6.98496900	-0.46641700	-1.33070500
N	9.94017000	0.22842600	0.55253400
N	14.96296200	-0.21836600	-0.33023700
C	2.63024100	0.45394800	0.61959900
H	2.00498900	0.82518500	1.42184600
C	4.01582000	0.46284000	0.71890300
H	4.46828500	0.85365200	1.62427000
C	4.78789800	-0.02574800	-0.34758000
C	6.25375800	-0.04654100	-0.31732500
C	8.29620800	-0.36749500	-1.01849700
C	8.62805900	0.12845300	0.23918200
C	10.67223300	-0.18990700	-0.46023800
C	12.14015800	-0.20828700	-0.43592100
C	12.90838600	-0.68569800	-1.50960100
H	12.44996800	-1.06965300	-2.41598500
C	14.29915500	-0.66843200	-1.40669400
H	14.90720600	-1.03519200	-2.23042400
C	14.22218500	0.23692900	0.69477800
H	14.77127500	0.59894300	1.56109200
C	12.82931100	0.26432300	0.69446100
H	12.28599100	0.64478200	1.55193600
C	4.10445800	-0.50448800	-1.47939100
H	4.65163900	-0.89262500	-2.33008000
C	2.71709000	-0.47485600	-1.50396800
H	2.14623800	-0.80948000	-2.36059200
O	0.05808300	-1.99481900	-0.68929300
O	-0.01346900	-1.00912100	1.25172300
O	-0.02441800	1.75416200	0.14610400
H	-12.27555500	-1.14290800	-2.24740400
C	-14.19375300	-0.85941000	-1.30398100
H	-14.75769200	-1.23796900	-2.15351200
O	-0.10587100	3.01246400	-1.79896700
C	-0.06498100	2.91799200	-0.56357100
C	-0.07468700	4.15130100	0.29924100
C	-0.12633700	5.41593100	-0.30680600
H	-0.15724900	5.48119000	-1.38967700
C	-0.13814500	6.58083600	0.45872400
H	-0.17878600	7.55409000	-0.02536800
C	-0.09770100	6.49043800	1.85711900
C	-0.04569300	5.23564100	2.47958500
H	-0.01487300	5.18050500	3.56396600
C	-0.03454700	4.07991600	1.70241700
H	0.00602800	3.10928100	2.18501300
O	-0.10650000	7.59271900	2.66725400
O	-0.04928300	-7.18026800	2.84849300
C	-0.03834600	-5.92030500	2.32897200
C	0.00279800	-5.80516500	0.93065100
H	0.02406900	-6.70524600	0.32381800
C	0.01556000	-4.54479400	0.34537500
H	0.04678000	-4.45060400	-0.73530000
C	-0.01268600	-3.38576800	1.14199700
C	-0.00024400	-2.04969500	0.52251500
C	-0.05381400	-3.51435100	2.54007400
H	-0.07605200	-2.62291300	3.15862700
C	-0.06645600	-4.77203000	3.13570200
H	-0.09760600	-4.86592300	4.21859500
H	-0.07759100	-7.14858700	3.81986200
H	-0.14258700	8.40463800	2.13388600
O	0.07896100	0.41830200	-2.33446900

FCG-11+ OOH*
E = -4394.487996

Co	-0.05712800	0.00254600	-0.59388500
S	9.68180000	-0.95898600	-1.84601300
S	7.10154800	0.41570800	1.09159400
N	1.92391800	-0.02551800	-0.51444900
N	6.91297500	-0.61879300	-1.31717500
N	9.86924300	0.07526200	0.56428400
N	14.88797300	-0.48463400	-0.27594500
C	2.56325400	0.42618000	0.57959400
H	1.94022800	0.81454400	1.37530400
C	3.94749700	0.40596700	0.69198200
H	4.39900500	0.79321800	1.59934600
C	4.71940600	-0.10670100	-0.36303300
C	6.18397600	-0.15651300	-0.32070500
C	8.22376800	-0.53565700	-0.99947500
C	8.55737200	-0.01026900	0.24589700
C	10.59925900	-0.38431900	-0.43197900
C	12.06649600	-0.42778500	-0.39851300
C	12.83269500	-0.92735700	-1.46352400
H	12.37324200	-1.31009100	-2.36991100
C	14.22293200	-0.93273800	-1.35245900
H	14.82946600	-1.31656700	-2.16949600
C	14.14911700	-0.00788300	0.74063700
H	14.69921300	0.35218200	1.60712200
C	12.75692100	0.04310100	0.73178400
H	12.21516800	0.43988500	1.58281900
C	4.03585000	-0.58155000	-1.49624400
H	4.58139200	-0.98913400	-2.33874800
C	2.65007900	-0.52279200	-1.53320300
H	2.09082900	-0.86255100	-2.39629800
O	-0.06167300	-1.95428400	-0.61776600
O	-0.11163200	-0.88994600	1.28283400

N	-1.95244200	-0.06997600	-0.58337800
S	-7.14382500	-0.75703200	-2.03554700
S	-9.70076700	0.33554800	1.03772500
N	-14.92208900	-0.29415300	-0.42608500
N	-9.90820500	-0.58036100	-1.41822900
N	-6.93498300	0.15913900	0.41909200
C	-14.24959700	0.18000200	0.63450800
H	-14.85098400	0.53546700	1.46802300
C	-12.85804600	0.23555100	0.70953700
H	-12.39229000	0.63915200	1.60354200
C	-12.09855300	-0.22760600	-0.37652000
C	-10.63047300	-0.20555800	-0.38169600
C	-8.59314900	-0.45019300	-1.12919900
C	-8.24918300	0.02603600	0.13283700
C	-6.21378800	-0.21399500	-0.61948500
C	-4.74788300	-0.17964300	-0.62507800
C	-3.98394500	-0.64210200	-1.70889600
H	-4.44471200	-1.05970000	-2.59804500
C	-2.59767000	-0.56855900	-1.65188300
H	-1.96711000	-0.88967500	-2.47100900
C	-2.66910400	0.36959700	0.46838100
H	-2.10294700	0.76153400	1.30410300
C	-4.05616600	0.33529700	0.48569700
H	-4.59538100	0.70640500	1.34890000
C	-12.79683100	-0.72478400	-1.49064600
H	-12.26048500	-1.09562800	-2.35668900
C	-14.18967500	-0.73493900	-1.46338000
H	-14.74579100	-1.11670700	-2.31662900
O	-0.10357700	3.03462800	-1.71725400
C	-0.07804500	2.89180700	-0.47754000
C	-0.11104600	4.09508600	0.42219000
C	-0.17608100	5.37963200	-0.13924700
H	-0.20029800	5.48326000	-1.21924400
C	-0.21039100	6.51598200	0.66750000
H	-0.26143800	7.50571500	0.21898100
C	-0.17896200	6.37580700	2.06212900
C	-0.11350000	5.10037200	2.64011200
H	-0.08989500	5.00718700	3.72204700
C	-0.08045100	3.97393300	1.82231000
H	-0.03021200	2.98674800	2.26909800
O	-0.20972900	7.44763700	2.91125100
O	0.03407000	-7.16770300	3.06462900
C	0.03088900	-5.92254700	2.50987900
C	0.06317900	-5.84661100	1.10865600
H	0.08924700	-6.76322200	0.52725100
C	0.06120100	-4.60315800	0.48797400
H	0.08568300	-4.53913000	-0.59510300
C	0.02671900	-3.42229100	1.25142700
C	0.02363500	-2.10478800	0.59240600
C	-0.00530000	-3.51168400	2.65267600
H	-0.03216700	-2.60345000	3.24610800
C	-0.00293000	-4.75212700	3.28380600
H	-0.02684200	-4.81509700	4.36910200
H	0.00999400	-7.10951500	4.03488400
H	-0.25435800	8.27777500	2.40749300
O	0.06684100	0.33218800	-2.35966100
H	0.00087900	1.30934900	-2.40153900

O	-0.06712800	1.82349100	0.03585000
N	-2.02603700	-0.01121500	-0.62668000
S	-7.22703100	-0.85136600	-1.95669700
S	-9.76080900	0.53862400	1.01391200
N	-14.98958700	-0.33462500	-0.29143500
N	-9.98568000	-0.64153100	-1.32500000
N	-7.00056700	0.32903900	0.38075100
C	-14.30700900	0.15224900	0.75687600
H	-14.89972300	0.49596600	1.60145600
C	-12.91554500	0.23209200	0.80744600
H	-12.44090700	0.63655200	1.69640600
C	-12.16729500	-0.21701900	-0.29222400
C	-10.70007500	-0.17057100	-0.32283500
C	-8.66921600	-0.46173400	-1.07118400
C	-8.31638100	0.15283100	0.12700400
C	-6.28718600	-0.14946800	-0.61927200
C	-4.82159900	-0.11095900	-0.64241000
C	-4.06510100	-0.71438700	-1.66018800
H	-4.53163500	-1.24364400	-2.48449000
C	-2.67891700	-0.64298300	-1.61721600
H	-2.05914700	-1.08692300	-2.38569600
C	-2.73524900	0.57142300	0.35796600
H	-2.16251000	1.07099600	1.12914100
C	-4.12245900	0.54564500	0.38565800
H	-4.65579000	1.02926200	1.19514100
C	-12.87614300	-0.72857400	-1.39307900
H	-12.34874600	-1.08875300	-2.26905000
C	-14.26787200	-0.76397800	-1.34094400
H	-14.83211100	-1.15607600	-2.18411500
O	0.67270200	3.12201300	-1.66252700
C	0.34647800	2.94124300	-0.46590300
C	0.41275100	4.08432200	0.50425600
C	0.78561000	5.36030300	0.05355200
H	1.02074500	5.50243000	-0.99616700
C	0.85643500	6.43989200	0.93214600
H	1.14544400	7.42391500	0.56998900
C	0.55095000	6.25092500	2.28740800
C	0.17738300	4.98319800	2.75508900
H	-0.05569600	4.85165200	3.80773600
C	0.11083600	3.91345900	1.86679600
H	-0.17753700	2.93232600	2.22857500
O	0.59944200	7.26689900	3.20098000
O	-0.18067300	-6.97462900	3.33186500
C	-0.16358800	-5.75167900	2.73027100
C	-0.13167800	-5.72970900	1.32704800
H	-0.12263000	-6.66808500	0.78094000
C	-0.11189800	-4.51117200	0.65919200
H	-0.08701100	-4.48965600	-0.42550500
C	-0.12327600	-3.30151700	1.37715900
C	-0.09878300	-2.00958200	0.67052800
C	-0.15659000	-3.33679300	2.78080700
H	-0.16618500	-2.40620800	3.33910200
C	-0.17646700	-4.55195400	3.45866900
H	-0.20127000	-4.57249100	4.54538700
H	-0.19972100	-6.88047300	4.29953000
H	0.86594800	8.09680600	2.77049600
O	-0.70842200	1.26657700	-2.97342200
H	-0.16447200	2.03588700	-2.64820200
O	0.04146100	0.17283200	-2.43423500

FCG-11+ H*
E= -4244.096066

Co	-0.02167900	0.00623300	-0.25530900
S	-9.68485100	-1.20780400	-1.72131200
S	-7.23944800	1.00741700	0.78678500

	N	-1.98626800	0.02756700	-0.26183000
	N	-6.94238900	-0.73920200	-1.15464400
	N	-9.98108900	0.54085400	0.21982300
	N	-14.95744000	-0.20649500	-0.72136500
	C	-2.67800400	0.78670300	0.60810100
	H	-2.08895500	1.38972300	1.28771700
	C	-4.06702200	0.81291300	0.63623000
	H	-4.55770300	1.44759100	1.36681900
	C	-4.79342800	0.02791500	-0.27298300
	C	-6.25873700	0.00861700	-0.31107900
	C	-8.26647100	-0.54887800	-0.96262400
	C	-8.65602300	0.34764400	0.02858200
	C	-10.66555900	-0.20600800	-0.62304900
	C	-12.13291000	-0.22207600	-0.67222400
	C	-12.85170300	-1.05233100	-1.54685600
	H	-12.35301000	-1.73041500	-2.23292300
	C	-14.24553800	-1.00594500	-1.53130600
	H	-14.81556500	-1.64354600	-2.20308400
	C	-14.26391200	0.58572500	0.11406300
	H	-14.85156500	1.22907000	0.76508600
	C	-12.87265400	0.61724100	0.17886700
	H	-12.36922800	1.27962400	0.87382100
	C	-4.05958700	-0.76183700	-1.17600600
	H	-4.56686100	-1.38685300	-1.90100200
	C	-2.67355700	-0.73625700	-1.13603900
	H	-2.08123600	-1.33940000	-1.81267500
	O	0.08602400	2.92560900	-1.69016900
	O	0.02755800	1.82741300	0.28987500
	O	0.02068900	-1.13431600	1.65314900
	N	1.93661500	-0.04359800	-0.37568200
	S	7.06376600	-1.07143400	-1.88025700
	S	9.76059800	0.68886200	0.72871600
	N	14.90772400	-0.33785000	-0.78064600
	N	9.85327200	-0.78273300	-1.44817400
	N	6.96847700	0.40005500	0.29560900
	C	14.28785900	0.31720100	0.21368500
	H	14.92925900	0.79828200	0.94849000
	C	12.90154700	0.40364000	0.34028300
	H	12.48015500	0.95322400	1.17667200
	C	12.08986300	-0.22421400	-0.61766400
	C	10.62319700	-0.18474200	-0.56154400
	C	8.55329600	-0.57262800	-1.13966300
	C	8.26809300	0.19077000	-0.01100500
	C	6.20012700	-0.20020500	-0.59173200
	C	4.73580800	-0.16079200	-0.53456900
	C	3.92340000	-0.83826600	-1.45840500
	H	4.34232800	-1.42994500	-2.26561300
	C	2.54212100	-0.75911600	-1.34287700
	H	1.89143700	-1.27975900	-2.03429800
	C	2.70525400	0.61118200	0.51683000
	H	2.17813700	1.17876700	1.27373300
	C	4.09224800	0.57595000	0.47492500
	H	4.66853500	1.11593700	1.21658500
	C	12.73298500	-0.91169800	-1.66167000
	H	12.15499000	-1.41394900	-2.42903100
	C	14.12543600	-0.93674700	-1.69494600
	H	14.63909900	-1.46386900	-2.49580000
	O	-0.05499300	-1.94234200	-0.39057100
	C	-0.01536600	-2.14225100	0.88630600
	C	-0.01184500	-3.53109300	1.40742000
	C	-0.04283700	-4.62858400	0.53202100
	H	-0.07058800	-4.45716200	-0.53909100
	C	-0.03712200	-5.93207700	1.02348000
	H	-0.06091200	-6.77681100	0.33877800
	C	0.00011000	-6.14954100	2.40867900
	C	0.03012200	-5.06279500	3.29534400
	H	0.05812100	-5.24965200	4.36472700

	C	0.02420200	-3.76592800	2.79298000
	H	0.04780200	-2.92112400	3.47400200
	O	0.00906000	-7.40086500	2.95476300
	O	0.20209400	7.82511400	2.39264400
	C	0.17248500	6.61273900	1.75767200
	C	0.17333400	6.62085100	0.35586200
	H	0.19765000	7.57052600	-0.17099500
	C	0.14247800	5.41486200	-0.33956200
	H	0.14253900	5.41645200	-1.42483300
	C	0.10969700	4.18467700	0.33866800
	C	0.07314800	2.89860400	-0.44755800
	C	0.11050500	4.19623100	1.74237600
	H	0.08654500	3.25576200	2.28240400
	C	0.14202100	5.39645400	2.45289600
	H	0.14250700	5.38821800	3.54062900
	H	0.19496900	7.70252600	3.35691600
	H	-0.00963400	-8.07593400	2.25554900
	H	-0.06269100	0.33122200	-1.66277800

References:

1. APEX2, v. 2014.7-1; Bruker AXS: Madison, WI, 2014.
2. SAINT, v. 8.34A; Bruker AXS: Madison, WI, 2013.
3. SADABS, v. 2014/3; Bruker AXS: Madison, WI, 2013.
4. O. V. Dolomanov, L. J. Bourhis, R. J. Gildea, J. A. K. Howard and H. Puschmann, *J. Appl. Crystallogr.*, 2009, **42**, 339-341.
5. A. Spek, *J. Appl. Crystallogr.*, 2003, **36**, 7-13.
6. V. A. Blatov, A. P. Shevchenko and D. M. Proserpio, *Cryst. Growth Des.*, 2014, **14**, 3576-3586.
7. A. D. Becke, *J. Chem. Phys.*, 1993, **98**, 5648-5652.
8. J. Tirado-Rives and W. L. Jorgensen, *Journal of Chemical Theory and Computation*, 2008, **4**, 297-306.
9. V. A. Rassolov, J. A. Pople, M. A. Ratner and T. L. Windus, *J. Chem. Phys.*, 1998, **109**, 1223-1229.
10. G.A. ;e. al. Frisch, M. J.; Trucks, G. W.; Schlegel, H. B.; Scuseria, G. E.; Robb, M. A.; Cheeseman, J. R.; Scalmani, G.; Barone, V.; Mennucci, B.; Petersson, Gaussian 09, revision D.01; Gaussian Inc.: Wallingford, CT, 2009., (n.d.).
11. P. J. Hay and W. R. Wadt, *J. Chem. Phys.* , 1985, **82**, 299-310.
12. S. Miertuš, E. Scrocco and J. Tomasi, *Chem. Phys.*, 1981, **55**, 117-129.
13. J. K. Nørskov, J. Rossmeisl, A. Logadottir, L. Lindqvist, J. R. Kitchin, T. Bligaard and H. Jónsson, *J. Phys. Chem. B*, 2004, **108**, 17886-17892.
14. J. Jiang, L. Huang, X. Liu and L. Ai, *ACS Appl. Mater. Interfaces*,2017, **9**, 7193-7201.
15. A. Rana, A. Karmakar, S. Kundu and S. Biswas, *Inorg. Chem.*, 2025, **64**, 6214-6223.
16. N. Seal, K. Karthick, M. Singh, S. Kundu and S. Neogi, *Chem. Eng. J.*, 2022, **429**, 132301.
17. X. Zhou, X. Shen, Z. Xia, Z. Zhang, J. Li, Y. Ma and Y. Qu, *ACS Appl. Mater. Interfaces*, 2015, **7**, 20322-20331.

18. W. Cheng, Z.-P. Wu, D. Luan, S.-Q. Zang and X. W. Lou, *Angew. Chem. Int. Ed.*, 2021, **60**, 26397-26402.
19. L. Yang, L. Zhang, G. Xu, X. Ma, W. Wang, H. Song and D. Jia, *ACS Sustainable Chem. Eng.*, 2018, **6**, 12961-12968.
20. A. Goswami, D. Ghosh, V. V. Chernyshev, A. Dey, D. Pradhan and K. Biradha, *ACS Appl. Mater. Interfaces*, 2020, **12**, 33679-33689.
21. J.-Q. Shen, P.-Q. Liao, D.-D. Zhou, C.-T. He, J.-X. Wu, W.-X. Zhang, J.-P. Zhang and X.-M. Chen, *J. Am. Chem. Soc.*, 2017, **139**, 1778-1781.
22. Y. Xu, B. Li, S. Zheng, P. Wu, J. Zhan, H. Xue, Q. Xu and H. Pang, *J. Mater. Chem. A*, 2018, **6**, 22070-22076.
23. Y. Liao, Y. Xiao, Z. Li, X. Zhou, J. Liu, F. Guo, J. Li and Y. Li, *small*, 2024, **20**, 2307685.
24. P. Dong, Y. Gu, G. Wen, R. Luo, S. Bao, J. Ma and J. Lei, *small*, 2023, **19**, 2301473.
25. Q. Qiu, T. Wang, L. Jing, K. Huang and D. Qin, *Int. J. Hydrogen Energy*, 2020, **45**, 11077-11088.
26. X. Hou, Z. Han, X. Xu, D. Sarker, J. Zhou, M. Wu, Z. Liu, M. Huang and H. Jiang, *Chem. Eng. J.*, 2021, **418**, 129330.
27. R. Chand, A. Karmakar, S. Kundu and S. Neogi, *Small*, 2024, **20**, 2404085.
28.S. Naik Shreyanka, J. Theerthagiri, S. J. Lee, Y. Yu and M. Y. Choi, *Chem. Eng. J.*, 2022, **446**, 137045.
29. E. Saha, K. Karthick, S. Kundu and J. Mitra, *J. Mater. Chem. A*2021, **9**, 26800-26809.
30. K. Ge, S. Sun, Y. Zhao, K. Yang, S. Wang, Z. Zhang, J. Cao, Y. Yang, Y. Zhang, M. Pan and L. Zhu, *Angew. Chem. Int. Ed.*, 2021, **60**, 12097-12102.
31. Z. Xu, C.-L. Yeh, Y. Jiang, X. Yun, C.-T. Li, K.-C. Ho, J. T. Lin and R. Y.-Y. Lin, *ACS Appl. Mater. Interfaces*, 2021, **13**, 28242-28251.
32. S. K. Konavarapu, G. Kim, K. Shin and S. Y. Kim, *Chem. Eur. J.*, 2025, **31**, e202500010.
33. P. Suresh, U. Rajaji, A. Natarajan, K. Rajagopal, A. A. Alothman and T.-Y. Liu, *Chem. Phys. Lett.*, 2024, **847**, 141371.
34. J. Wang, L. Wang, R. Wu, C. Fan, X. Zhang and Y. Fan, *Inorg. Chem.*, 2024, **63**, 11542-11553.
35. M.-R. Liu, Q.-L. Hong, Q.-H. Li, Y. Du, H.-X. Zhang, S. Chen, T. Zhou and J. Zhang, *Adv. Funct. Mater.*, 2018, **28**, 1801136.
36. H. Huang, S. Zhou, C. Yu, H. Huang, J. Zhao, L. Dai and J. Qiu, *Energy Environ. Sci.*, 2020, **13**, 545-553.
37. H. Jiang, Z. Zhao, G. Li, M. Wang, P. Chen, X. Liu, X. Tu, Y. Hu, Z. Shen and Y. Wu, *Adv. Sci.*, 2024, **11**, 2306919.
38. A. Gupta, C. A. Allison, M. E. Ellis, J. Choi, A. Davis, R. Srivastava, F. M. de Souza, D. Neupane, S. R. Mishra, F. Perez, A. Kumar, R. K. Gupta and T. Dawsey, *Int. J. Hydrogen Energy* 2023, **48**, 9551-9564.
39. D. Zhu, J. Liu, Y. Zhao, Y. Zheng and S.-Z. Qiao, *Small*, 2019, **15**, 1805511.

40. T. I. Singh, G. Rajeshkhanna, U. N. Pan, T. Kshetri, H. Lin, N. H. Kim and J. H. Lee, *Small*, 2021, **17**, 2101312.
41. S. J. Patil, N. R. Chodankar, S.-K. Hwang, P. A. Shinde, G. Seeta Rama Raju, K. Shanmugam Ranjith, Y. S. Huh and Y.-K. Han, *Chem. Eng. J.*, 2022, **429**, 132379.
42. D. C. Cha, T. I. Singh, A. Maibam, T. H. Kim, D. H. Nam, R. Babarao and S. Lee, *Small*, 2023, **19**, 2301405.
43. Y. Yuan, K. Wang, B. Zhong, D. Yu, F. Ye, J. Liu, J. Dutta and P. Zhang, *Energy Environ. Mater.*, 2024, **7**, e12747.
44. J. Wu, D. Wang, S. Wan, H. Liu, C. Wang and X. Wang, *Small*, 2020, **16**, 1900550.
45. Y. Liu, P. Li, Z. Wang and L. Gao, *Materials*, 2024, **17**, 2195.
46. Q. Liang, H. Jin, Z. Wang, Y. Xiong, S. Yuan, X. Zeng, D. He and S. Mu, *Nano Energy*, 2019, **57**, 746-752.
47. B. You, N. Jiang, M. Sheng, S. Gul, J. Yano and Y. Sun, *Chem. Mater.*, 2015, **27**, 7636-7642.
48. N. Diyali, S. Diyali, M. Chettri, S. Saha, S. K. Agrawalla, H. Bagdwal, C. S. Purohit, M. Singh and B. Biswas, *ACS Appl. Mater. Interfaces*, 2025, **17**, 9351-9363.
49. S. Sk, R. Madhu, D. S. Gavali, V. Bhasin, R. Thapa, S. N. Jha, D. Bhattacharyya, S. Kundu and U. Pal, *J. Mater. Chem. A*, 2023, **11**, 10309-10318.
50. C. Lin, D. Wang, H. Jin, P. Wang, D. Chen, B. Liu and S. Mu, *J. Mater. Chem. A*, 2020, **8**, 4570-4578.
51. C. Wang, J. Jiang, T. Ding, G. Chen, W. Xu and Q. Yang, *Adv. Mater. Interfaces*, 2016, **3**, 1500454.